FERMILAB-PUB-11-221-PPD

Measurement of K^+ production cross section by 8 GeV protons using high energy neutrino interactions in the SciBooNE detector

G. Cheng,[3] C. Mariani,[3] J. L. Alcaraz-Aunion,[1] S. J. Brice,[4] L. Bugel,[13] J. Catala-Perez,[18] J. M. Conrad,[13] Z. Djurcic,[3] U. Dore,[15] D. A. Finley,[4] A. J. Franke,[3] C. Giganti,[15,a] J. J. Gomez-Cadenas,[18] P. Guzowski,[6] A. Hanson,[7] Y. Hayato,[8] K. Hiraide,[10,8] G. Jover-Manas,[1] G. Karagiorgi,[13] T. Katori,[7,13] Y. K. Kobayashi,[17] T. Kobilarcik,[4] H. Kubo,[10] Y. Kurimoto,[10,5] W. C. Louis,[11] P. F. Loverre,[15] L. Ludovici,[15] K. B. M. Mahn,[3,b] S. Masuike,[17] K. Matsuoka,[10] V. T. McGary,[13] W. Metcalf,[12] G. B. Mills,[11] G. Mitsuka,[9,c] Y. Miyachi,[17,d] S. Mizugashira,[17] C. D. Moore,[4] Y. Nakajima,[10,e] T. Nakaya,[10] R. Napora,[14] P. Nienaber,[16] D. Orme,[10] M. Otani,[10] A. D. Russell,[4] F. Sanchez,[1] M. H. Shaevitz,[3] T.-A. Shibata,[17] M. Sorel,[18] R. J. Stefanski,[4] H. Takei,[17,f] H.-K. Tanaka,[13,g] M. Tanaka,[5] R. Tayloe,[7] I. J. Taylor,[6,h] R. J. Tesarek,[4] Y. Uchida,[6] R. Van de Water,[11] J. J. Walding,[6,i] M. O. Wascko,[6] H. B. White,[4] M. Yokoyama,[10,j] G. P. Zeller,[4] and E. D. Zimmerman[2]

(SciBooNE Collaboration)

[1] *Institut de Fisica d'Altes Energies, Universitat Autonoma de Barcelona, E-08193 Bellaterra (Barcelona), Spain*
[2] *Department of Physics, University of Colorado, Boulder, Colorado 80309, USA*
[3] *Department of Physics, Columbia University, New York, New York 10027, USA*
[4] *Fermi National Accelerator Laboratory; Batavia, Illinois 60510, USA*
[5] *High Energy Accelerator Research Organization (KEK), Tsukuba, Ibaraki 305-0801, Japan*
[6] *Department of Physics, Imperial College London, London SW7 2AZ, United Kingdom*
[7] *Department of Physics, Indiana University, Bloomington, Indiana 47405, USA*
[8] *Kamioka Observatory, Institute for Cosmic Ray Research, University of Tokyo, Gifu 506-1205, Japan*
[9] *Research Center for Cosmic Neutrinos, Institute for Cosmic Ray Research, University of Tokyo, Kashiwa, Chiba 277-8582, Japan*
[10] *Department of Physics, Kyoto University, Kyoto 606-8502, Japan*
[11] *Los Alamos National Laboratory, Los Alamos, New Mexico 87545, USA*
[12] *Department of Physics and Astronomy, Louisiana State University, Baton Rouge, Louisiana 70803, USA*
[13] *Department of Physics, Massachusetts Institute of Technology, Cambridge, Massachusetts 02139, USA*
[14] *Department of Chemistry and Physics, Purdue University Calumet, Hammond, Indiana 46323, USA*
[15] *Università di Roma Sapienza, Dipartimento di Fisica and INFN, I-00185 Rome, Italy*
[16] *Physics Department, Saint Mary's University of Minnesota, Winona, Minnesota 55987, USA*
[17] *Department of Physics, Tokyo Institute of Technology, Tokyo 152-8551, Japan*
[18] *Instituto de Fisica Corpuscular, Universidad de Valencia and CSIC, E-46071 Valencia, Spain*

(Dated: May 14, 2011)

The SciBooNE Collaboration reports K^+ production cross section and rate measurements using high energy daughter muon neutrino scattering data off the SciBar polystyrene (C_8H_8) target in the SciBooNE detector. The K^+ mesons are produced by 8 GeV protons striking a beryllium target in Fermilab Booster Neutrino Beam line (BNB). Using observed neutrino and antineutrino events in SciBooNE, we measure

$$\frac{d^2\sigma}{dpd\Omega} = (5.34 \pm 0.76)\ mb/(GeV/c \times sr)$$

for $p + Be \rightarrow K^+ + X$ at mean K^+ energy of 3.9 GeV and angle (with respect to the proton beam direction) of 3.7 degrees, corresponding to the selected K^+ sample. Compared to Monte Carlo predictions using previous higher energy K^+ production measurements, this measurement, which uses the NUANCE neutrino interaction generator, is consistent with a normalization factor of 0.85±0.12. This agreement is evidence that the extrapolation of the higher energy K^+ measurements to an 8 GeV beam energy using Feynman scaling is valid. This measurement reduces the error on the K^+ production cross section from 40% to 14%.

PACS numbers: 13.87.Eb, 13.20.-v, 13.15.+g

[a] Present address: DSM/Irfu/SPP, CEA Saclay, F-91191 Gif-sur-Yvette, France
[b] Present address: TRIUMF, Vancouver, British Columbia, V6T 2A3, Canada
[c] Present address: Solar-Terrestrial Environment Laboratory, Nagoya University, Furo-cho, Chikusa-ku, Nagoya, Japan
[d] Present address: Department of Physics, Yamagata University, Yamagata, 990-8560 Japan
[e] Present address: Lawrence Berkeley National Laboratory, Berkeley, CA 94720, USA
[f] Present address: Kitasato University, Tokyo, 108-8641 Japan
[g] Present address: Brookhaven National Laboratory, Upton, New

Operated by Fermi Research Alliance, LLC under Contract No. DE-AC02-07CH11359 with the United States Department of Energy

I. INTRODUCTION

Inclusive kaon production by low-energy protons (1 to 15 GeV) is of interest both theoretically and experimentally. In this low-energy region, kaon production is dominated by exclusive processes. For example, the lowest threshold K^+ production process is $p + p \rightarrow K^+ + \Lambda + p$, which for a fixed target setup has an incoming beam energy threshold of 2.52 GeV. Since exclusive channel threshold effects are important, theoretical models such as Feynman scaling [1] may be better in describing low-energy production cross sections. Measurements of kaon production in this region are not extensive and do not cover wide kinematic regions. In addition, systematic data on the energy and target nuclei dependence is not available. Thus, new measurements of kaon production are needed in this region. Experimentally, kaon production is also relevant for neutrino experiments since important components of the incident neutrino flux come from kaon decays.

A primary motivation of this work is to verify the simulation of neutrinos from the Fermilab Booster Neutrino Beam (BNB) line with actual data. The BNB line provides neutrinos for the MiniBooNE [2] and SciBooNE [3] experiments, as well as possible future experiments, including MicroBooNE [4]. In this beam line, protons with 8 GeV kinetic energy are directed onto a 1.8-interaction length beryllium target. The average energy of π^+ (K^+) that decay to neutrinos in the MiniBooNE detector acceptance is 1.89 (2.66) GeV. Therefore 37.6% (92.1%) decay before the end of the 50 m long decay region. The relevant decay modes for MiniBooNE/SciBooNE are $\pi^+ \rightarrow \mu^+\nu_\mu$, $K^+ \rightarrow \mu^+\nu_\mu$, which produce 92.9% of the neutrino beam, $\pi^- \rightarrow \mu^-\bar{\nu}_\mu$, which produces 6.5% of the neutrino beam, and $K^+ \rightarrow \pi^0 e^+\nu_e$, $\mu^+ \rightarrow e^+\bar{\nu}_\mu\nu_e$, $K^0_L \rightarrow \pi^- e^+\nu_e$, and $K^0_L \rightarrow \pi^+ e^-\bar{\nu}_e$, which produce 0.6% of the neutrino beam.

While the neutrino flux is predominantly due to π^+ decay, K^+ decay is the dominant source above 2 GeV. The neutrinos from kaons provide a unique source of high energy events for experiments on the BNB line studying neutrino cross sections, and can represent a source of background for experiments exploring neutrino oscillations and beyond-the-standard-model effects. Therefore, it is important for the BNB line experiments to understand the rate of K^+ production.

An accurate understanding of K^+ production will reduce systematics associated with the measured ν_e background in MiniBooNE, a major contributor to the uncertainty in the previously published ν_e oscillation appearance result [5]. The measurement of K^+ production in this energy region combined with K^+ production at higher energies is a good test of production models such as the Feynman-Scaling [6] and Modified Sanford-Wang [7] parameterization used to describe secondary meson production at low primary proton beam energy in the BNB.

This work describes a measurement of K^+ production by measuring the rate of high-energy ν_μ events from kaon decay. The data sample used for the measurement comes from the interaction of ν_μ and $\bar{\nu}_\mu$ which undergo charged current (CC) neutrino interactions in the fiducial volume of the SciBooNE detector, generating high energy μ^- and μ^+ (along with a host of other particles) that penetrate the entire SciBooNE detector, providing essentially a minimum muon momentum requirement of 1.0 GeV/c. The neutrinos from K^+ decay can be isolated using the angular distribution of the outgoing muons and the multiplicity of charged particles produced in the interaction. The number of K^+ decay neutrinos is then compared to prediction to make a determination of a normalization factor for production in the BNB and correspondingly a K^+ production cross section. The paucity of high-energy events in the SciBooNE experiment prevents a measurement of the kinematic distribution of K^+ production but does allow a normalization determination with improved uncertainty.

II. SCIBOONE EXPERIMENT

A. Neutrino Beam

The SciBooNE experiment detected neutrinos produced by the Fermilab BNB. The same BNB beam is also serving the MiniBooNE experiment. The BNB uses protons accelerated to 8 GeV kinetic energy by the Fermilab Booster synchrotron. Beam properties are monitored on a spill-by-spill basis, and at various locations along the BNB line. Transverse and directional alignment of the beam, beam width and angular divergence, beam intensity and losses along the BNB, are measured and used in the data quality selection. Protons strike a 71.1 cm long beryllium target, producing a secondary beam of hadrons, mainly pions with a small fraction of kaons. A cylindrical horn electromagnet made of aluminum surrounds the beryllium target to sign-select and focus the secondary beam. For neutrino running mode, the horn polarity was set to focus particles with positive electric charge and for antineutrino running mode, the horn polarity was set to focus particles with negative electric charge. The neutrino beam is mostly produced in the 50 m long decay region. The analysis described in this paper will use data from both neutrino and antineutrino running modes.

The Monte Carlo (MC) simulation of the neutrino

York 11973, USA
[h] Present address: Department of Physics and Astronomy, State University of New York, Stony Brook, New York 11794-3800, USA
[i] Present address: Department of Physics, College of William & Mary, Williamsburg, VA 23187, USA
[j] Present address: Department of Physics, University of Tokyo, Tokyo 113-0033, Japan

beam was modeled by the MiniBooNE collaboration. The MiniBooNE collaboration uses a GEANT4-based Monte Carlo simulation that can be roughly divided into five consecutive simulation steps. The first simulation step is the definition of the beam-line geometry including the shape, location, and composition of components. The second simulation step is the generation of primary protons according to the measured beam optics properties. The third simulation step is the simulation of particles produced by the initial p-Be interaction, including the elastic and quasi-elastic scattering of the protons in the target. Custom tables for the production of proton, neutron, $\pi^{\pm}$, $K^{\pm}$, K^0 are used based on the phenomenology of particle production and data of the production of these particles at higher energies. The fourth simulation step is the propagation of the produced particles using the GEANT4 framework taking into account energy loss, electromagnetic and hadronic processes, and trajectory deflection by the magnetic field created by the horn. The fifth simulation step is the decay of propagated particles into neutrinos using the current branching fraction measurements [2].

Particle production is simulated using the methods described in Ref. [2]. The production of K^+ is simulated using a Feynman scaling formalism based on K^+ p-Be production data at different primary proton energies [2, 6]. The predicted double differential cross section using the Feynman parametrization reported in [2, 6] is

$$\frac{d^2\sigma}{dpd\Omega} = (6.3 \pm 2.5)\ mb/(GeV/c \times sr), \qquad (1)$$

at the mean K^+ energy of 3.9 GeV and mean angle of 3.7 degrees, which are the mean energy and angle for kaons which produce neutrinos in SciBooNE.

For π^+ and π^- production, the Sanford-Wang (SW) [8] parametrization to the HARP p-Be data [9] at 8.89 GeV/c is used to determine the central value with associated errors determined from spline fits. SW [8] production is also used for K^0 production and errors. The long life time of the K^0_L combined with the fact that they are not focused by the magnetic horn leads to the expectation that the contribution of decay neutrinos for this source is small relative to the K^+. For K^- production, the scarcity of production measurements in the relevant kinematic regions motivated the use of the MARS hadronic interaction package [10] to determine the absolute double differential cross-sections.

The neutrinos produced from the simulation are extrapolated along straight lines toward the SciBooNE detector. All neutrinos whose ray traces cross any part of the detector volume and surrounding rock are considered in the SciBooNE neutrino flux prediction and the kinematics of the neutrino and their parents are stored.

In the neutrino mode running (positive horn polarity), a total neutrino flux of $2.2 \times 10^{-8}\mathrm{cm}^{-2}/\mathrm{POT}$ is expected at the SciBooNE detector location, with a mean neutrino energy of 0.7 GeV. The flux is dominated by muon neutrinos (92.92% of total), with small contributions from muon antineutrinos (6.48%), electron neutrinos (0.54%) and electron antineutrinos (0.05%).

In the antineutrino mode running (negative horn polarity), a total neutrino flux of $1.3 \times 10^{-8}\mathrm{cm}^{-2}/\mathrm{POT}$ is expected at the SciBooNE detector location, with a mean neutrino energy of 0.6 GeV. The flux is dominated by muon antineutrinos (83.85% of total), with contributions from muon neutrinos (15.58%), electron neutrinos (0.15%) and electron antineutrinos (0.42%).

The neutrino flux predictions at the SciBooNE detector location as a function of neutrino energy for both neutrino and antineutrino mode running are shown in Fig. 1.

The systematic uncertainties in the neutrino flux prediction come from several sources in the simulation steps above: proton delivery/optics, secondary particle productions, hadronic interactions in the target or horn and horn magnetic field. Fig. 2 shows the ν_μ flux in neutrino mode from π^+ and K^+ decays, and their fractional uncertainties. Fig. 3 shows the ν_μ and $\bar{\nu}_\mu$ flux in antineutrino mode from π^-, π^+, and K^+ decays, and their fractional uncertainties. The uncertainty in π^+ (π^-) production is determined from uncertainties associated with spline fits to the HARP π^+ (π^-) double differential cross section data [2] and differences between the SW and spline fit central values. The HARP data used were those from a thin (5% interaction length) beryllium target run [9]. While the HARP data provide a valuable constraint on the BNB flux prediction, additional uncertainties resulting from thick target effects (secondary re-scattering of protons and pions) are included through the BNB flux simulation. The resulting π^+ production uncertainty is $\approx 5\%$ at the peak of the flux distribution and increases significantly at high and low neutrino energies. The resulting π^- production uncertainty is $\approx 10\%$ at the peak of the flux distribution and also increases at high and low neutrino energies.

The flux from K^+ decay is dominant for $E_\nu > 2.0$ GeV. Since no published data exist for K^+ production at the BNB primary proton beam energy, we employ the Feynman scaling hypothesis to relate K^+ production measurements at different proton beam energies to the expected production at the BNB proton beam energy [2]. The errors of the Feynman scaling parameters obtained from these measurements are then included as systematic uncertainties.

Other major contributions to the flux error include uncertainties in the hadron interactions at the target and simulation of the the horn magnetic field, which both contribute to shape and normalization uncertainties. An overall normalization uncertainty is included on the number of protons on target (POT). All flux errors are modeled through variations in the simulation and result in a total error of $\approx 7\%$ at the peak of the flux. Quantitative constraints of each uncertainty have been determined from previous MiniBooNE studies [2].

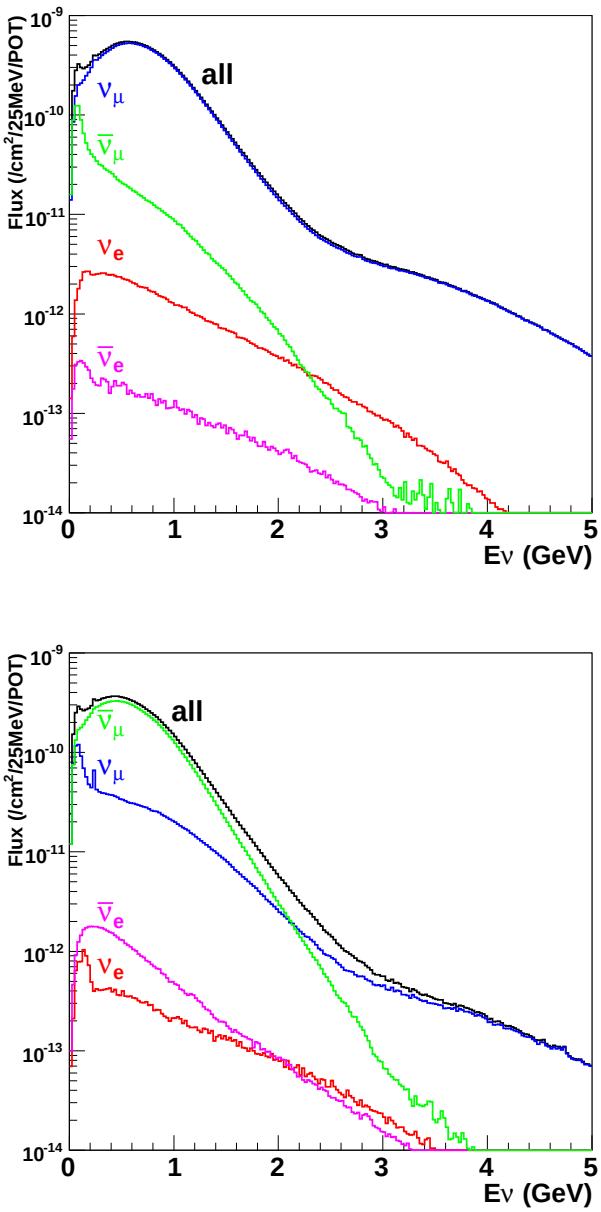

FIG. 1. Neutrino flux predictions at the SciBooNE detector as a function of neutrino energy E_ν, normalized per unit area, proton on target (POT), and neutrino energy bin width, in neutrino (top) and antineutrino (bottom) modes. The spectra is averaged within a circle with radius 2.12m from beam center (coincides with center of detector cross-sectional area), which covers the entire 3m×3m cross-sectional area of the SciBooNE detector. The total flux and contributions from individual neutrino flavors are shown.

B. SciBooNE Detector

The SciBooNE detector was located 100 m downstream from the beryllium target on the axis of the beam, as shown in Fig. 4. The detector was comprised of three sub-

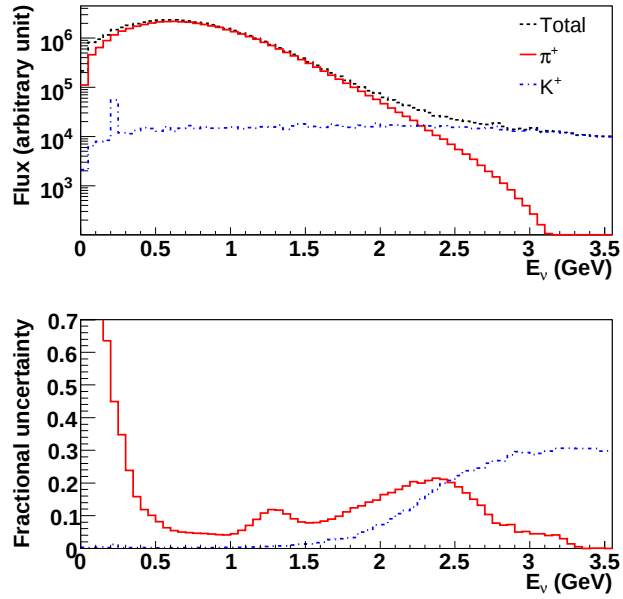

FIG. 2. (Top) ν_μ flux prediction at the SciBooNE detector as a function of neutrino energy E_ν in neutrino running mode. The total flux and contributions from π^+ and K^+ decays are shown. (Bottom) Fractional uncertainty of the ν_μ flux prediction due to π^+ and K^+ production from the p-Be interaction in neutrino running mode. The figures are from Ref. [11].

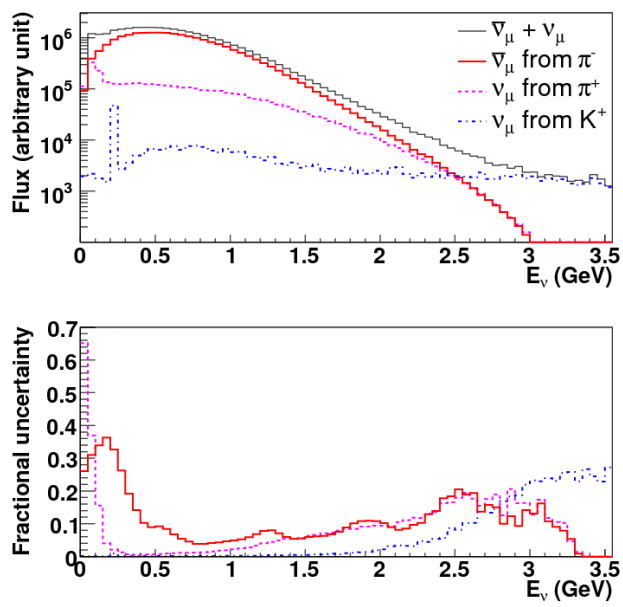

FIG. 3. (Top) ν_μ and $\bar{\nu}_\mu$ flux predictions at the SciBooNE detector as a function of neutrino energy E_ν in antineutrino running mode. The total flux and contributions from $\bar{\nu}_\mu$ from π^- decay and ν_μ from π^+ and K^+ decays are shown. (Bottom) Fractional uncertainty of the $\bar{\nu}_\mu$ flux prediction due to π^- production and ν_μ flux prediction due to π^+ and K^+ production from the p-Be interaction in antineutrino running mode.

detectors: a fully active and finely segmented scintillator tracker (SciBar), an electromagnetic calorimeter (EC), and a muon range detector (MRD). SciBar served as the primary neutrino target for this analysis.

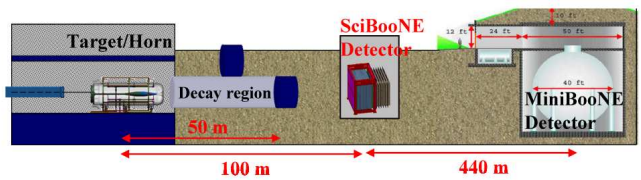

FIG. 4. Schematic overview of the Booster Neutrino Beamline and the location of the SciBooNE and the MiniBooNE detectors.

SciBooNE uses a right-handed Cartesian coordinate system in which the z axis is the beam direction and the y axis is the vertical upward direction. The origin is located on the most upstream surface of SciBar in the z dimension, and at the center of the SciBar scintillator plane in the x and y dimensions. Since each sub-detector is read out both vertically and horizontally, two views are defined: top (x vs. z projection) and side (y vs. z projection).

The SciBar detector [12] was positioned upstream of the other sub-detectors. It consists of 14,336 extruded plastic scintillator strips. Each strip has a dimension of $2.5 \times 300 \times 1.3$ cm^3. The scintillators are arranged vertically and horizontally to construct a $3 \times 3 \times 1.7$ m^3 volume with a total mass of 15 tons. The dominant component of the SciBar detector is polystyrene (C_8H_8). The uncertainty of the total detector mass is estimated to be 1%, including the effect of epoxy resin used to glue the strips.

Each strip was read out by a 64-channel multi-anode photo-multiplier (MA-PMT) via a wavelength shifting (WLS) fiber. Charge information was recorded for each channel, while timing information was recorded in groups of 32 channels by taking the logical OR with multi-hit TDC modules [13]. The timing resolution for minimum-ionizing particles was evaluated with cosmic ray data to be 1.6 ns. The average light yield for minimum-ionizing particles is approximately 20 photo-electrons per 1.3 cm path length, and the typical pedestal width is below 0.3 photo-electron. The hit finding efficiency evaluated with cosmic ray data is more than 99.8%. The minimum length of a reconstructable track is approximately 8 cm (three layers hit in each view). The track finding efficiency for single tracks of 10 cm or longer is more than 99%.

The EC is located just downstream of SciBar, and is designed to measure the electron neutrino contamination in the beam and tag photons from π^0 decay. The EC is a "spaghetti" type calorimeter comprised of 1 mm diameter scintillating fibers embedded in lead foil [14]. The calorimeter is made of 64 modules of dimensions $262 \times 8 \times 4$ cm^3. The fibers are bundled in two independent groups of 4×4 cm^2 transverse cross section, read at both ends by Hamamatsu PMTs.

The MRD was installed downstream of the EC and is designed to measure the momentum of muons produced by CC neutrino interactions. It comprised of 12 iron plates with thickness 5 cm sandwiched between planes of 6 mm thick scintillation counters; there were 13 alternating horizontal and vertical planes read out via 362 individual 2 inch PMTs. Each iron plate measured 274×305 cm^2. The MRD measured the momentum of muons up to 1.2 GeV/c using the observed muon range. Charge and timing information from each PMT were recorded. The average hit finding efficiency is 99%.

C. Detector Response Simulation

The GEANT4 framework is used for the detector simulation. The Bertini cascade model within GEANT4 [15] is used to simulate the interactions of hadronic particles with detector materials. The detector simulation includes a detailed geometric model of the detector, including the detector frame, experimental hall, and soil. The energy loss of a particle in each single SciBar strip and each individual EC sensitive fiber is simulated. The energy deposition is converted in the detector response taking into account the Birk's saturation of the scintillator, the light attenuation along the fibers, the Poisson fluctuation of the number of photoelectrons, the PMT resolution, and electronic noise. The crosstalk in nearby SciBar channels is also simulated.

In SciBar the timing of each hit is simulated from the true time of the corresponding energy deposition, corrected by the travel time of the light in the WLS fiber and smeared by the timing resolution.

For the detector simulation of the MRD, true energy deposition in each scintillator is converted to ADC counts using the conversion factor measured with cosmic muons. The attenuation of light in the scintillator as well as electronics noise are simulated. The time of energy deposition is digitized and converted into TDC counts.

The input parameters of the detector simulation are derived from laboratory measurements and calibration data. The features of the simulation have been systematically compared and tuned with cosmic ray and neutrino data.

A more detailed description of the detector simulation is given in [16].

D. Neutrino Interaction Simulation

In the SciBooNE experiment, neutrino interactions with carbon and hydrogen in the SciBar detector are simulated by the NEUT [17, 18] and NUANCE [19] program libraries. NEUT is used in Kamiokande, Super-Kamiokande, K2K, and T2K experiments, while NUANCE is used in MiniBooNE. Several Monte Carlo samples with different NEUT and NUANCE implementa-

tions are produced, and compared to the SciBooNE neutrino data. For the analysis presented in this paper we use NUANCE as the neutrino interaction simulation code because this Monte Carlo matches what was used in the MiniBooNE oscillation analysis [20]. The same analysis will also be repeated using NEUT and presented in Appendix B. The total number of protons on target (POT) collected in neutrino mode is 0.99×10^{20} while the POT for the antineutrino mode is 1.51×10^{20}. The expected number of events in the SciBooNE detector for each neutrino (antineutrino) interaction is listed in Tab. I.

TABLE I. The expected number of events in each neutrino interaction estimated by NUANCE at the SciBooNE detector location with the neutrino beam exposure of 0.99×10^{20} protons on target for neutrino mode and of 1.51×10^{20} for antineutrino mode. The 9.8 ton fiducial volume of the SciBar detector is assumed. Charged Current and Neutral Current interactions are abbreviated as CC and NC, respectively.

	NUANCE	
Interaction	# Events neutrino mode	# Events antineutrino mode
CC QE	45,163	15,361
CC single-π	24,437	6,413
CC coherent π	1,706	1,326
CC DIS+Other	3,049	1,518
NC	29,118	11,686

For neutrino mode beam exposure, the total number of CC interactions predicted by NUANCE integrated over the SciBooNE flux in the 9.8 ton SciBar fiducial volume is 7.44×10^4 for 0.99×10^{20} POT. For antineutrino mode beam exposure, the total number of CC interactions predicted by NUANCE integrated over the SciBooNE flux in the 9.8 ton SciBar fiducial volume is 2.46×10^4 for 1.51×10^{20} POT.

The targets handled in NUANCE are proton, neutron, and carbon nuclei. The types of neutrino interactions simulated in both Neutral Current (NC) and CC are: elastic and quasi-elastic scattering ($\nu N \rightarrow \ell N'$), single meson production ($\nu N \rightarrow \ell N' m$), single gamma production ($\nu N \rightarrow \ell N' \gamma$), coherent π production, and deep inelastic scattering ($\nu N \rightarrow \ell N' hadrons$), where N and N' are the nucleons (proton or neutron), ℓ is the lepton (electron, muon or neutrino), and m is the meson. NUANCE also simulates resonantly-produced multi-pion and kaon production ($K^+\Lambda$, $K^+\Sigma$). In nuclei, interactions of the mesons and hadrons with the nuclear medium are simulated following the neutrino interactions.

In addition to neutrino interactions inside SciBar, we also simulate interactions in the EC and MRD and the surrounding materials (the walls of the detector hall and soil).

1. Quasi-elastic Scattering

The dominant interaction in SciBooNE is CC quasi-elastic scattering, which is implemented using the Smith and Moniz model [21]. The nucleons are treated as quasi-free particles with Fermi motion and Pauli blocking taken into account. The Fermi surface momentum (p_F) for carbon is set to 220 MeV/c and the nuclear potential (E_B) is set to 34 MeV/c, as extracted from electron scattering data [22] taking into account neutrino vs. electron scattering differences [23]. For the vector form factor, NUANCE uses the BBA-2003 form factor [24] with a dipole form for the axial form factor with an adjustable axial mass, M_A^{QE} for Carbon (M_A^{QE}-C) and for Hydrogen (M_A^{QE}-H). The M_A^{QE}-H is used only in the antineutrino mode running. In NUANCE, an empirical Pauli-blocking parameter, κ is introduced [25] to better describe the MiniBooNE quasi-elastic data at low momentum transfer. When $\kappa > 1$, the Pauli-blocking of final state nucleons is increased and hence the cross section at low momentum transfer is suppressed. The values of (M_A^{QE}-C = 1.234, M_A^{QE}-H = 1.0) GeV/c^2 and $\kappa = 1.022$ are used [23]. The same Fermi momentum distribution and nuclear potential are used in all other neutrino-nucleus interactions except for coherent π production.

2. Meson Production via Baryon Resonances

The second most frequent interaction in SciBooNE is the resonant production of single pion, kaon, and eta mesons which NUANCE described with the model of Rein and Sehgal [26]. The Rein and Sehgal model assumes an intermediate baryon resonance, N^*, in the reaction of $\nu N \rightarrow \ell N^*, N^* \rightarrow N' m$. All intermediate baryon resonances with mass less than 1.7 GeV/c^2 are included. Interactions with invariant masses greater than 2 GeV/c^2 are simulated as deep inelastic scattering. Δ re-interactions ($\Delta N \rightarrow NN$) which do not lead to a mesonic final state are also simulated. This re-interaction probability is assumed to be 10% (20%) for $\Delta^{++/-}$ ($\Delta^{+/0}$) resonances. To determine the angular distribution of final state pions, the method of [27] is used for the $P_{33}(1232)$ resonance. For other resonances, the directional distribution of the generated pion is chosen to be isotropic in the resonance rest frame. The axial-vector form factors are formalized to be dipole with $M_A^{1\pi} = 1.10$ GeV/c^2.

3. Coherent Pion Production

Coherent pion production is a neutrino interaction with a nucleus which remains intact, releasing one pion with the same charge as the incoming weak current. Because of the small momentum transfer to the target nucleus, the outgoing pion tends to be emitted in the for-

ward direction, closely following the incoming neutrino direction. The formalism developed by Rein and Sehgal [28, 29] is used to simulate such interactions. The axial vector mass, $M_A^{coherent}$, is set to 1.03 ± 0.28 GeV/c^2. The total and inelastic pion-nucleon cross sections from the original Rein-Sehgal publications [28, 29] are obtained from fits to PDG data and implemented as a function of pion energy. The Rein and Sehgal model predicts the CC coherent π^+ production rate to be approximately 1% of the total neutrino CC rate in SciBooNE.

4. Deep Inelastic Scattering

The deep inelastic scattering (DIS) cross section is calculated using the GRV98 parton distribution functions [30]. Additionally, we have included the corrections in the small Q^2 region developed by Bodek and Yang [31]. The DIS contribution slowly increases for W values starting at 1.7 GeV and becomes the only source of neutrino interactions above W>2 GeV. This is done to create a smooth transition between the resonance and DIS models and ensure continuity in distributions of kinematics and hadron multiplicity in the region of overlap. Tab. II summarizes the parameter choices used in NUANCE.

TABLE II. NUANCE parameters used for neutrino interaction simulation.

p_F	220 MeV
E_B	34 MeV
M_A^{QE}-C	1.234 GeV
M_A^{QE}-H	1.0 GeV
κ	1.022
$M_A^{1\pi}$	1.10 GeV
$M_A^{coherent}$	1.03 GeV
$M_A^{N\pi}$	1.3 GeV

5. Intra-nuclear Interactions

Following production, the intra-nuclear interactions of mesons and nucleons are simulated using a cascade model in which the particles are traced until they escape the target nucleus.

Although we only use kinematic information from the final state muon in this analysis, the simulation of intern-uclear interaction is important since the pions/protons emitted from the nucleus can affect the selection criteria and bias the kinematics of the final state muon.

Inelastic scattering, charge exchange and absorption of pions in nuclei are simulated. For inelastic scattering and charge exchange interactions, the direction and momentum of pions are affected. In the scattering amplitude, Pauli blocking is also taken into account. A more detailed description of the intra-nuclear interaction simulations in NUANCE can be found in [19].

III. NEUTRINO MODE ANALYSIS

In this analysis, we use a sample of high energy ν_μ events identified by muons penetrating the SciBar, EC, and MRD detectors. According to our Monte Carlo simulation, 43% of these high energy neutrinos come from K^+ decays in the beam.

The entire neutrino-mode data set for the SciBooNE experiment is used for this analysis. The neutrino run occurred from October 2007 to April 2008. A total of 0.99×10^{20} POT, after all data quality cuts, was collected with an efficiency of 95%.

The hit threshold in SciBar is set at 2.5 photoelectrons (corresponding to roughly 0.25 MeV) for a scintillator strip. The hits in each view are then associated into two-dimensional (2D) tracks in each view using a cellular automaton algorithm developed in K2K [32]. First, a correction for cross talk is applied to both data and MC prediction before 2D track reconstruction. Then, the remaining hits are categorized into "clusters", where a cluster is one or more hits in adjacent scintillator strips. Segments are formed, which connect individual clusters no more than one scintillator strip apart. Any segments which share a cluster are then connected, provided the χ^2 of a least squares linear fit remains acceptable. Three dimensional tracks are formed from 2D tracks in both views by requiring the timing between the 2D tracks to be within 50 ns, and the start and end point in the z direction for the 2D tracks to be within 6.6 cm.

A reconstructed muon track (referred to as a SciBar-MRD matched track) consists of a SciBar reconstructed track matching a reconstructed track in the MRD. The fiducial volume (FV) is applied requiring the upstream edge of the track to be within $|x| \leq 130$ cm, $|y| \leq 130$ cm, and $5.24 \leq |z| \leq 149.34$ cm. This corresponds to a 9.7 m^3 FV and 9.8 tons of fiducial mass. This selection criterion is not the same as is used in previous SciBooNE publications of 10.6 tons; the selection has been optimized for the particular analysis here. As only MRD events are selected, a muon-hypothesis track selection is unnecessary, and the FV selection has been modified to boost the number of events in the sample without adding backgrounds. The track is also required to be in time with the neutrino beam, i.e. within $0 \leq t \leq 2,000$ ns. The extrapolation of the SciBar track is required to be matched with a track in MRD within 30 cm and within a 100 ns time difference. The matching requires a track that penetrates at least four consecutive MRD layers. If no MRD track is found, MRD hits can be used for the matching. The MRD hits, which in this case are required to be within a cone with an aperture of ± 0.5 rad, should have a time within 100 ns with respect to the SciBar track and should be within 10 cm of the extrapolated SciBar track on the MRD first layer.

The SciBar-MRD matched track can be further classified based on the end point of the MRD matched track: if the SciBar-MRD matched track stops in the MRD, the track is defined as SciBar-MRD stopped. If the track goes through all of the MRD planes, the track is classified as SciBar-MRD penetrated. If the SciBar-MRD matched track escapes from the side of the MRD before the most downstream plane, the event is classified as SciBar-MRD side-escaped.

In this analysis we will consider only events with one SciBar-MRD penetrated track. This defines a sample enriched in high energy muon neutrino events. The selected muons will have a minimum momentum of 1.0 GeV/c and muon angle relative to beam axis of less than 45 degrees.

The data sets for SciBooNE are subject to contamination by cosmic backgrounds (due to lack of detector shielding or veto). The vast majority of the cosmic backgrounds come from cosmic muons, which can mimic a muon signal from a ν_μ interaction in SciBar. The selection cuts remove most of the cosmic background muons due to differences between cosmic background muons and muons created by neutrino beam interactions. The FV and timing cuts in SciBar remove the cosmic backgrounds coming from outside the detector and beam window. Most of the cosmic backgrounds enter the detector from above, producing vertical tracks (neutrino beam event tracks are generally horizontal). The vertical cosmic tracks do not pass through both SciBar and MRD and no SciBar-MRD matched track can be reconstructed, failing the cut requiring a SciBar-MRD matched track. For events with a SciBar-MRD matched track, the cosmic background contamination in the beam timing window is 0.5%, estimated using a beam-off timing window ($5,000 \leq t \leq 15,000$ ns). To further correct for the cosmic backgrounds, identical selection cuts are made in data in the timing region $5,000 \leq t \leq 15,000$ ns, far outside the beam timing window and 5 times as long for better statistics. The data numbers and distributions selected in this cosmic background region are then divided by 5 and subtracted from the corresponding data events and distributions selected in the beam timing window. The resulting cosmic background subtracted data numbers and distributions assume no further cosmic background contamination. There is no cosmic background modeling in the MC. The number of events from cosmic backgrounds, neutrino interactions in the EC and MRD, and events with neutrino interactions in the material surrounding the SciBar detector are negligible. For all three samples combined, the number of background events is estimated to be 26 events: 15 from cosmic, 9 from backscattering neutrino events in EC/MRD, and 2 from interaction outside the SciBooNE detectors.

The high energy muons penetrate through the entire SciBooNE detector so the reconstruction of the total muon energy could not be done. The reconstructed muon angle relative to beam axis will be used as the primary kinematic variable for the analysis. Neutrinos produced from K^+ decay have a higher energy on average than neutrinos from π^+ decay. Therefore, the angular distribution of the resulting muon from the neutrino interaction of a neutrino from K^+ will be more forward peaked than those from neutrinos from π^+.

After all the previously mentioned selection cuts, the resulting data and MC samples are further divided into three separate samples based on the number of SciBar reconstructed tracks in each event. The number of SciBar reconstructed tracks for data and MC (along with its different contributions) can be seen in Fig. 5. The SciBar 1-Track sample contains mostly (78%) CCQE interactions, the SciBar 2-Track sample contains both CCQE(46%) and CC1π (42%) and the SciBar 3-Track sample contains mostly CC1π(62%) events together with QE and DIS interactions. The reconstructed muon angle distributions for the SciBar 1, 2 and 3-Track samples are shown in Fig. 6. Fig. 6 shows an excess in the MC events with respect to the data for low angle muon reconstructed tracks which is largely attributed to the difficulty in correctly modeling nuclear final state interactions. We believe that this MC/data discrepancy at low reconstructed muon angle is due to modeling of proton emission; the effect is covered by the uncertainty included for the modeling in Sec. V.

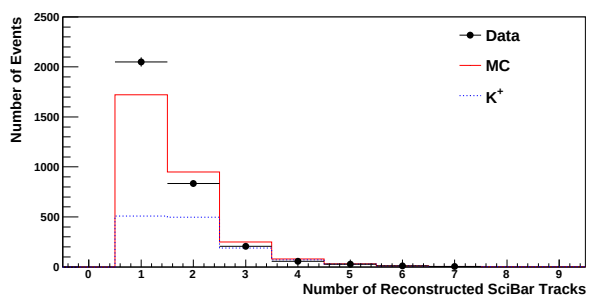

FIG. 5. Number of SciBar reconstructed tracks for the selected event sample in neutrino mode for data and NUANCE MC. MC histogram includes all events and K^+ shows the component of ν_μ from K^+.

Tab. III shows the number of events coming from K^+, π^+, data, and MC (NUANCE) along with efficiencies and purities (defined in Eqs. 2, 3) for the three selected samples.

We define the efficiency and purity using MC simulated events as:

$$\epsilon_{K^+} = \frac{\#\ selected\ events}{\#\ generated\ K^+}, \tag{2}$$

$$\pi_{K^+} = \frac{\#\ true\ K^+\ in\ selected\ sample}{\#\ selected\ events}, \tag{3}$$

The mean energy and mean angle (with respect to proton beam direction) of the selected K^+ and the mean energy for ν_μ from the selected K^+ in each of the three samples is summarized in Tab. IV. Fig. 7 shows the 2-dimensional distribution of K^+ production angle relative

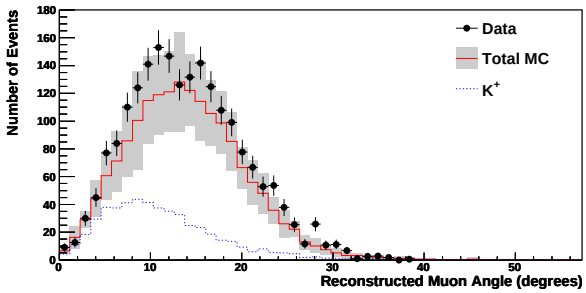

(a) 1-Track Sample

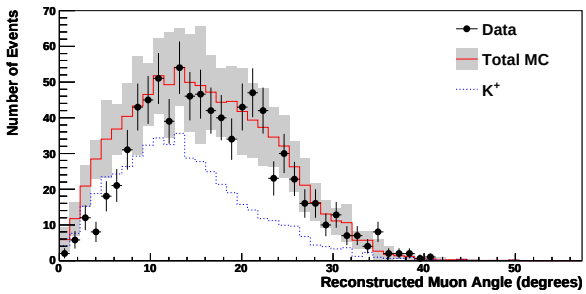

(b) 2-Track Sample

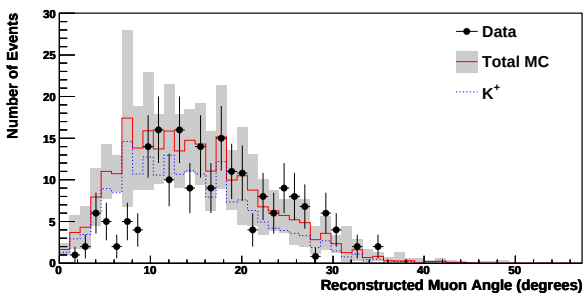

(c) 3-Track Sample

FIG. 6. Reconstructed muon angle for the SciBar 1-Track, 2-Track, and 3-Track samples in the neutrino mode analysis. The background contributions from K^- and K_L^0 are very small but included in the MC histogram.

to proton beam axis versus true K^+ production energy for predicted K^+ events selected in the SciBar 1-Track, 2-Track and 3-Track MC samples for the neutrino mode analysis.

The background from K^- and K_L^0 decays are very small. The expected number of K^- and K_L^0 events predicted for all three samples combined are 5 and 3 events, respectively.

IV. ANTINEUTRINO MODE ANALYSIS

The dataset used in this analysis consists of antineutrino-mode events collected between June 2007 and August 2008 corresponding to a total of 1.51×10^{20} POT, after all data quality cuts. The data collection efficiency was also 95% in this case.

The majority of events in antineutrino mode running are $\bar{\nu}_\mu$ from π^- decay, with a significant ν_μ contribution coming from the decay of positively charged π^+ and K^+. At higher energies (above 2 GeV), the positively charged "wrong-sign" particles, mainly π^+ and K^+, are strongly boosted in the forward direction, traveling downstream nearly parallel to the beam axis direction, such that they are not defocused by the magnetic horn. These particles create a 40% background of wrong sign neutrino interactions in the antineutrino mode run. In this analysis, we select a sample of high energy ν_μ coming from K^+. The analysis strategy is very similar to what is described in Sec. III with the difference that the background composition in the selected sample is different. Background events result from high energy ν_μ from π^+ produced in the initial p-Be interaction, and the decay of π^- (also produced in the initial p-Be interaction) that generate high energy $\bar{\nu}_\mu$. Both the ν_μ and $\bar{\nu}_\mu$ result in high energy muons (with negative and positive charge respectively) that penetrate the SciBar, EC and MRD detec-

TABLE III. Number of events for data and for NUANCE MC after selection cuts for the neutrino mode analysis. MRD indicates the SciBar-MRD sample, and MRD pen. stands for SciBar-MRD penetrated sample. The cosmic backgrounds have been subtracted from the data. The first column contains the number of predicted events with a ν_μ coming from $K+$ while the second column contains the number of predicted events with a ν_μ coming from π^+. The third column and fourth column represent the number of events in data and MC and the last two columns are the efficiency ($\epsilon(K^+)$) and purity ($\pi(K^+)$) for ν_μ from K^+ in MC. The total event prediction from simulation is labeled as MC.

Event Sel.	$K^+\nu_\mu$	$\pi^+\nu_\mu$	Data	MC	$\epsilon(K^+)$	$\pi(K^+)$
MRD	2,867	18,173	27,049	22,142	58%	13%
MRD pen.	1,508	1,700	3,365	3,286	31%	46%
Single μ	1,313	1,666	3,188	3,053	27%	43%
1-Trk	509	1,159	2,050	1,723	10%	30%
2-Trk	497	438	834	950	10%	52%
3-Trk	189	57	206	250	4%	76%

TABLE IV. Nuance MC predicted mean energy and mean angle (with respect to the proton beam direction) for the selected K^+ samples and predicted MC energy for the selected ν_μ from K^+ for the three SciBar samples in neutrino mode running. Errors correspond to the RMS of the relative distributions.

	E_{K^+} (GeV)	θ_{K^+}(degree)	E_{ν_μ} (GeV)
1-Track	3.6±1.2	4.3±2.1	3.0±1.0
2-Track	3.8±1.2	4.1±2.0	3.3±1.0
3-Track	4.1±1.1	3.9±1.9	3.5±0.9

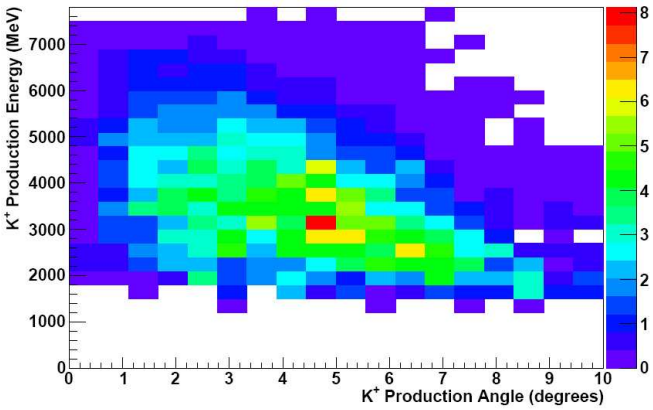

(a) 1-Track Sample

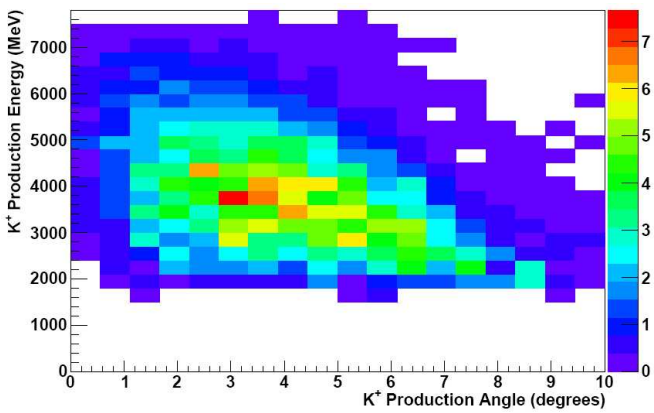

(b) 2-Track Sample

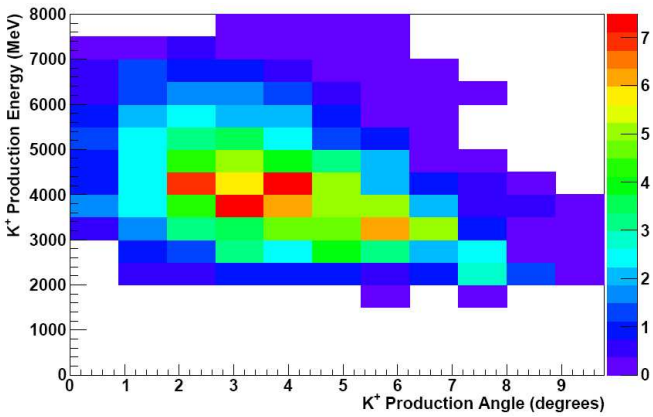

(c) 3-Track Sample

FIG. 7. Two-dimensional plots of the energy vs angle relative to the proton beam axis for the K^+ selected events in the SciBar 1-Track, 2-Track, and 3-Track MC samples for the neutrino mode analysis.

tors. Positive and negative muons are indistinguishable in SciBooNE due to the lack of magnetic field in our detector system.

As in the neutrino mode analysis, events passing the base selection cuts are further divided into three samples based on whether the events contain 1, 2 or 3 SciBar reconstructed tracks. The number of SciBar reconstructed tracks for data and MC (along with the parent) can be seen in Fig. 8. The SciBar 1-Track sample contains mostly (81%) charged current quasi-elastic interaction events. The SciBar 2-Track sample is evenly split between charged current quasi-elastic(40%) and charged current resonant pion interactions (44%), with a tiny contribution from charged current multi-π/DIS interactions (6%). The SciBar 3-Track sample contains mostly charged current resonant pion interactions (61%), with small contributions from charged current quasi-elastic (12%) and charged current multi-π/DIS interactions (21%). The reconstructed muon angle distributions for the SciBar 1, 2 and 3-Track samples are shown in Fig. 9. In this case the ν_μ events coming from K^+ have high energies, peaking at smaller angles, while the lower energy π^+ and π^- background distributions are spread more evenly across a broader range of angles.

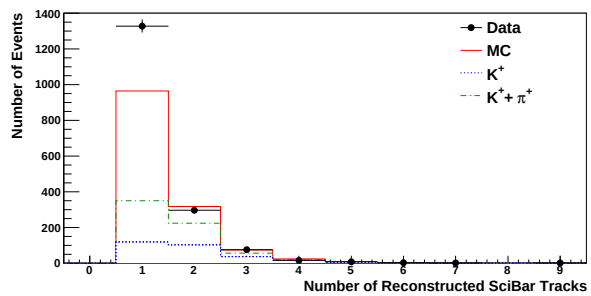

FIG. 8. Number of SciBar reconstructed tracks for the selected event sample in antineutrino mode for data and NUANCE MC. MC histogram includes all events and K^+ shows the component of ν_μ from K^+ and $K^+ + \pi^+$ shows the component of ν_μ from K^+ and π^+.

In this analysis, we also found a slight disagreement between data and Monte Carlo at low angle regions for the SciBar 2 and 3-Track samples for the reconstructed muon angle (see Fig. 9). This disagreement is caused, as in the ν_μ analysis, by the imperfect modeling of nuclear and intra-nuclear interactions in our neutrino interaction simulation program.

Tab. V summarizes the selected number of events in Data and MC (NUANCE) for the three selected samples, together with the efficiency and purity of K^+ (defined in Eqs. 2, 3) .

The mean energy and mean angle (with respect to the proton beam direction) for the selected K^+ and the mean energy for ν_μ from the selected K^+ in each of the three samples is summarized in Tab. VI. Fig. 10 shows the 2-dimensional distribution of K^+ production angle relative to proton beam axis versus true K^+ production energy for predicted K^+ events selected in the SciBar 1-Track, 2-Track and 3-Track MC samples for the antineutrino mode analysis. As can be seen in Fig. 10, the K^+ are much more forward than in neutrino mode (Fig. 7) otherwise they would have been swept out by the horn.

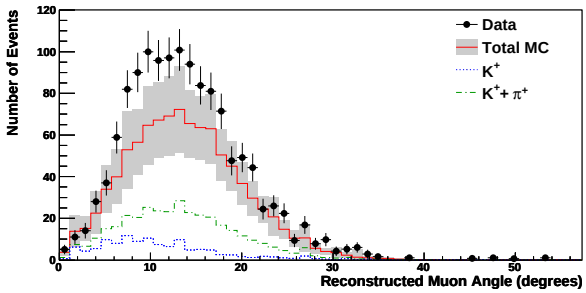

(a) 1-Track Sample

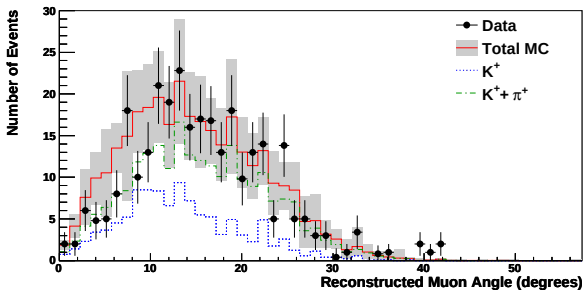

(b) 2-Track Sample

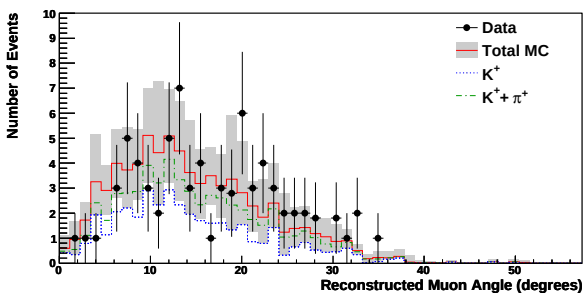

(c) 3-Track Sample

FIG. 9. Reconstructed muon angle for the SciBar 1-Track, 2-Track, and 3-Track sample in the antineutrino mode analysis. The background contributions from K^- and K_L^0 are small but included in the MC histogram.

The number of neutrinos coming from K^- and K_L^0 decays are small: the number of expected K^- and K_L^0 events predicted for all three samples combined are 25 and 5 events, respectively. Fig. 11 shows the reconstructed muon angle for the 2-Track sample with the K^- and K_L^0 contributions. Interactions from cosmic backgrounds, neutrino interactions in the EC and MRD, and events with neutrino interactions in the material surrounding the SciBar detector make a negligible contribution in this analysis as well. For all three samples combined, 19 events are estimated from cosmic backgrounds, 1 event is estimated from backscattering neutrino events in EC and MRD, and 3 events are estimated from neutrino interactions outside the SciBooNE detector.

TABLE V. Number of events for data and for NUANCE MC after selection cuts for the antineutrino mode analysis. MRD indicates the SciBar-MRD sample, and MRD pen. stands for SciBar-MRD penetrated sample. The cosmic backgrounds have been subtracted from the data. The first column contains the number of predicted events with ν_μ coming from $K+$, the second column contains the number of predicted events with ν_μ coming from π^+, and the third column contains the number of predicted events with $\bar{\nu}_\mu$ coming from π^-. Fourth column and fifth column represent the number of events in data and MC and the last two columns are the efficiency ($\epsilon(K^+)$) and purity ($\pi(K^+)$) for ν_μ from K^+ in MC. The total event prediction from simulation is labeled as MC.

Event Sel.	$K^+\nu_\mu$	$\pi^+\nu_\mu$	$\pi^-\bar{\nu}_\mu$	Data	MC	$\epsilon(K^+)$	$\pi(K^+)$
MRD	705	2,287	6,167	11,528	9,499	52%	7%
MRD pen.	326	385	698	1,790	1,452	24%	22%
Single μ	283	375	691	1,728	1,389	21%	20%
1-Trk	119	230	589	1328	965	9%	12%
2-Trk	103	121	83	296	317	8%	32%
3-Trk	36	19	15	75	74	3%	49%

TABLE VI. Nuance MC predicted mean energy and mean angle (with respect to the proton beam direction) for the selected K^+ samples and predicted MC energy for the selected ν_μ from K^+ for the three SciBar samples in antineutrino mode running. Errors correspond to the RMS of the relative distributions.

	E_{K^+} (GeV)	θ_{K^+}(degree)	E_ν (GeV)
1-Track	4.1±1.2	2.4±1.8	3.1±1.1
2-Track	4.4±1.2	1.9±1.4	3.4±1.0
3-Track	4.6±1.1	1.6±1.0	3.6±1.0

V. SYSTEMATIC UNCERTAINTIES

Systematic uncertainties are included by using a covariance matrix that includes the correlated and uncorrelated errors among the muon angle bins in the SciBar 1, 2, 3-Track samples. The covariance matrix is determined by calculating the correlated event changes for a given systematic uncertainty and then combining these (the different systematic uncertainties are assumed to be uncorrelated) to form the matrix. Statistical errors are also included as uncorrelated terms in the diagonal elements.

A. Neutrino Beam Uncertainties

The uncertainties in the delivery of the primary proton beam to the beryllium target and the primary beam optics, secondary hadron production in proton-beryllium interactions, hadronic interactions in the target and horn

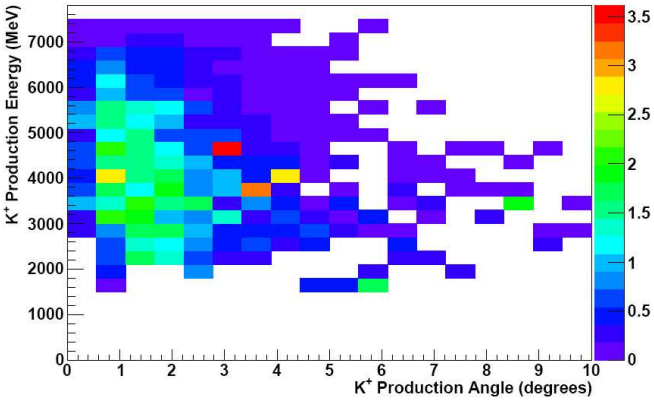

(a) 1-Track Sample

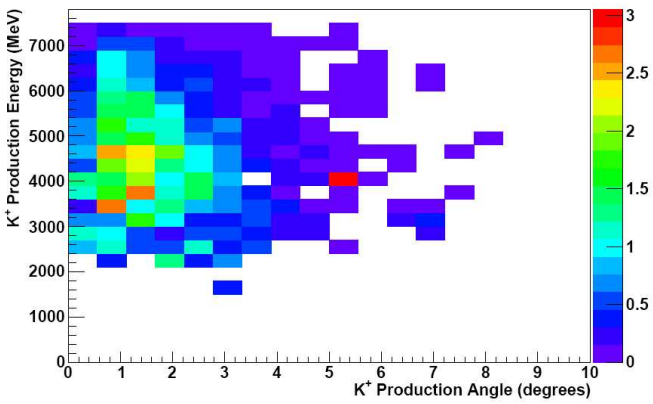

(b) 2-Track Sample

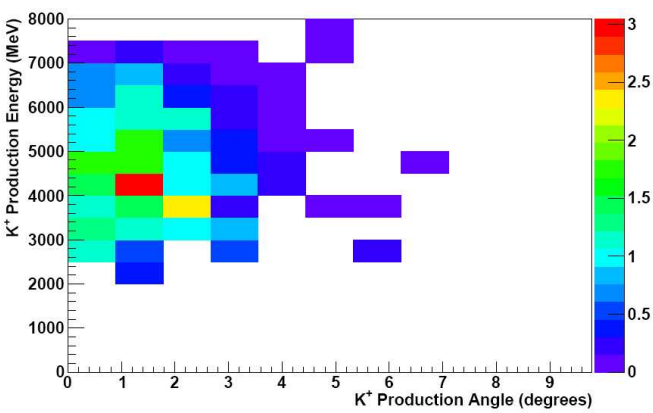

(c) 3-Track Sample

FIG. 10. Two-dimensional plots of the energy vs angle relative to the proton beam axis for the K^+ selected events in the SciBar 1-Track, 2-Track, and 3-Track MC samples for the antineutrino mode analysis. The K^+ are much more forward than in neutrino mode (Fig. 7) otherwise they would have been swept out by the horn, this can be seen also in the angular distribution difference between Tab. IV and Tab. VI.

and the horn magnetic field model are considered. The change in the neutrino beam spectrum due to these uncertainties is calculated by drawing random parameter vectors (all the beam systematics are varied within their

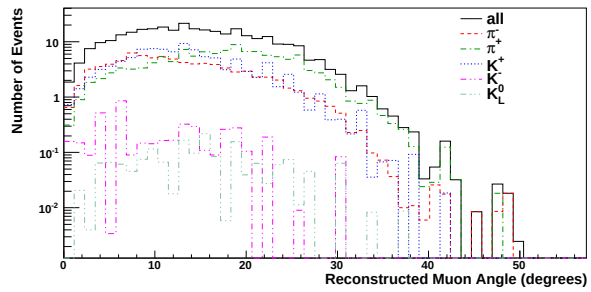

FIG. 11. The various meson contributions that decay into ν_μ and $\bar{\nu}_\mu$ as a function of reconstructed muon angle in the 2-Track sample in antineutrino mode.

uncertainties when drawing random parameter vectors) and weighting each event by a factor corresponding to the variation of the yield of the parent meson with the given momentum and angle.

To evaluate the neutrino beam uncertainties for both the neutrino and antineutrino mode running, a thousand random parameter vectors are generated, resulting in a thousand neutrino beam flux predictions and a thousand individual weights for each MC event. The thousand individual sets of weights for the MC simulation are passed through each analysis resulting in a thousand individual outcomes for each analysis. The correlated event changes associated with the thousand individual outcomes are used to form the error matrix for the beam systematic uncertainties.

For K^- production error, which is not accounted for in the previous neutrino beam uncertainty weights, a conservative 100% production uncertainty is applied.

B. Detector Uncertainties

1. *PMT Crosstalk and Resolution*

The crosstalk of the MA-PMT was measured to be 3.15% for adjacent channels, with an absolute error of 0.4% [16]. The single photoelectron resolution of the MA-PMT is set to 50% in the simulation, and the absolute error is estimated to be ±20%. Several complete MC simulation sets, with the crosstalk level and single photoelectron resolution separately varied within their uncertainties, are prepared and the changes in the final results using the varied MC simulation sets are taken as the systematic uncertainties.

2. *Scintillator Quenching*

Birk's constant for the SciBar scintillator was measured to be 0.0208 ± 0.0023 cm/MeV [16] and is varied within the measurement to evaluate the systematic error.

3. Hit Threshold

The conversion factors from the ADC counts to the photoelectron were measured for all 14,336 MA-PMT channels in SciBar. The measurement uncertainty was at the 20% level. Since the number of photoelectrons (2.5 p.e.) for the SciBar hit threshold was used, the hit threshold is varied by ±20% to evaluate the systematic error for SciBar track reconstruction.

4. TDC Dead time

The TDC dead time is set to 55 ns in the MC simulation, with the error estimated to be ±20 ns [33]. A MC simulation set with variations in the TDC dead time was prepared to determine the systematic error.

C. Cross section and nuclear model uncertainties

1. CC Quasi Elastic Scattering Cross Section

A systematic uncertainty of ±0.234 GeV is assigned to the M_A^{QE}-C to span the difference between the value used and the value from the global fit to historical data [34]. The difference between $\kappa = 1.000$ and $\kappa = 1.022$ is also assigned as a systematic uncertainty and added in quadrature to the M_A^{QE}-C error. M_A^{QE}-H error gives a negligible contribution.

2. CC Resonant Pion Production Cross Section

From a previous K2K measurement [35], the uncertainty in the resonant pion scattering cross section is estimated to be ±20%. An additional uncertainty is assigned to account for the observed Q^2 disagreement between the SciBooNE CC 1π-enriched data samples and the MC [11]. The uncertainty is evaluated by re-weighting CC resonant pion events as a function of true Q^2 such that they match the observed distribution in the SciBooNE data. Resonance decays leading to multi-pion final states are also included in the model and are simulated assuming $M_A^{N\pi} = 1.30$ GeV/c^2. This value of $M_A^{N\pi}$ is chosen strictly to ensure that the total CC cross section prediction reproduces previous experimental data.

3. Multi Pion Production and Deep Inelastic Scattering Cross Section

The uncertainties for multi pion and deep inelastic scattering (DIS) cross sections are set respectively at ±40%. The 40% multi-pion and DIS uncertainties come from a comparison of the NUANCE predictions to the existing multi-pion data in [36, 37].

4. Pion Interaction in the Initial Target Nucleus

For pions produced by neutrino interactions, uncertainties on the cross sections for pion absorption, pion inelastic scattering, and pion charge exchange in the nucleus are considered. The values of absorption, inelastic scattering, and charge exchange for pions are varied by ±30% in the MC independently while keeping the total number of neutrino events with pion processes fixed to determine the systematic uncertainties of each process.

5. Proton Emission

A systematic uncertainty associated with the emission of a proton following pion absorption in the nucleus is also included. The proton emission uncertainty covers the discrepancy between data and MC at low angles. The uncertainty is calculated for both NUANCE and NEUT, with NEUT giving the larger uncertainty, so the uncertainty is conservatively estimated using NEUT.

VI. FITS TO DETERMINE THE K^+ PRODUCTION AND RATE NORMALIZATION

The final state reconstructed track multiplicity and the muon angular distributions for the selected high energy events are different for neutrinos produced by pion and kaon decays as presented in Sec. III and in Sec. IV. Therefore, we fit these distributions in order to isolate neutrinos from kaon decays and minimize the following χ^2 function:

$$\chi^2 = \chi^2_\nu + \chi^2_{\bar{\nu}} = \sum_{i,j}^{N}(N_i^{obs} - N_i^{pred})(V^{\nu}_{stat} + V^{\nu}_{sys})^{-1}_{ij}(N_j^{obs} - N_j^{pred}) + \sum_{p,q}^{M}(M_p^{obs} - M_p^{pred})(V^{\bar{\nu}}_{stat} + V^{\bar{\nu}}_{sys})^{-1}_{pq}(M_q^{obs} - M_q^{pred}). \quad (4)$$

Cross section values (CCQE and CC1π for ν and $\bar{\nu}$) and uncertainties are included in the fit as described respectively in Appendix A and in Sec. V.

Two separate K^+ normalizations with respect to the beam MC predictions (Eq. 1) are extracted from the K^+ selected samples, a K^+_{prod}, the K^+ production flux at the beam target, and a K^+_{rate}, the $K^+_{prod}\times$ neutrino cross-sections. These two types of determinations are needed since the K^+_{prod} normalization can be used to determine a measured K^+ production cross section and the K^+_{rate} normalization can be used by BNB experiments as better estimates of the K^+ production rate in their beam.

The χ^2 function in Eq. 4 contains two terms: the former χ^2_ν term is associated with events for neutrino mode running and the latter $\chi^2_{\bar{\nu}}$ term is associated with events

for antineutrino mode running. The two χ^2 functions are assumed to be effectively uncorrelated since the cross section uncertainties for the antineutrino mode data are small compared to the statistical and background uncertainties. In the neutrino mode running, all three samples (SciBar 1, 2, 3-Track) are used simultaneously in the fit including their correlated bin-to-bin uncertainties. Only bins with 10 or more events are included in the χ^2. N and M are the number of bins used in the three reconstructed angle distributions in neutrino and antineutrino mode, respectively. $N^{obs}_{i(j)}$ and $N^{pred}_{i(j)}$ are the numbers of observed and predicted events in the $i(j)$-th angle bin for the neutrino mode analysis. $M^{obs}_{p(q)}$ and $M^{pred}_{p(q)}$ are the same quantities for the antineutrino in the $p(q)$-th angle bin.

For the K+ production analysis, the functions that describe the number of predicted events $N^{pred}_{i(j)}$ and $M^{pred}_{p(q)}$ are given by Eq. A1 for neutrinos and Eq. A3 for antineutrinos in Appendix A. $(V^{\nu}_{sys})_{ij}$ and $(V^{\bar{\nu}}_{sys})_{pq}$ are the elements of the covariance matrix for neutrino and antineutrino mode for each of the systematic uncertainties described in Sec. V. V^{ν}_{stat} ($V^{\bar{\nu}}_{stat}$) represents the statistical error in neutrino mode running (antineutrino mode running). An initial neutrino mode and antineutrino mode combined χ^2 minimization is performed to determine the best cross-section normalization factors for both ν_μ and $\bar{\nu}_\mu$ as described in Appendix A. Pull terms on the cross-sections normalization factors are added to keep the minimization physical. After the initial combined χ^2 minimization, the cross-section weights are fixed in N^{pred}_i and M^{pred}_p at their minimized values and the pull terms are removed from the χ^2 to evaluate the total (statistical+systematical) uncertainty on the K^+ production or rate. These cross-section weights are initially minimized to allow for better agreement between data and MC in the plots and do not affect either K^+ production or rate weights because the large uncertainties on the neutrino cross-section values are already taken into account in the covariance matrix.

TABLE VII. Summary of the fit results for the cross-section normalization factors as described in Appendix A with respect to NUANCE predictions. The top four values are cross section normalization values for ν_μ and $\bar{\nu}_\mu$ coming from π^+ and K^+ while the last two are normalization factors for $\bar{\nu}_\mu$ coming from π^-.

π^+/K^+		Fit Value
	CCQE in ν mode	1.17±0.14
	CCQE in $\bar{\nu}$ mode	1.07±0.25
	CC1π in ν mode	0.89±0.25
	CC1π in $\bar{\nu}$ mode	0.91±0.26
π^-		
	CCQE in $\bar{\nu}$ mode	1.50±0.21
	CC1π in $\bar{\nu}$ mode	1.49±0.29

The K^+ rate is measured by minimizing the same χ^2 function as described in Eq. 4 but using Eq. A2 and Eq. A4 respectively for neutrino and antineutrino to predict the number of events. A summary of the cross section normalizations is presented in Tab. VII. Many of these values are consistent with low energy precision cross-section measurements from the MiniBooNE experiment [2, 38–40] though the two sets of cross-section values are measured at different energies. The MiniBooNE collaboration measures cross-sections at neutrino energies less than 2 GeV while the cross-section values listed in Tab. VII are at neutrino energies greater than 3 GeV (as could be seen from Tab. IV and Tab. VI).

A summary of the fit results obtained for the K^+ production and rate separately for the neutrino, antineutrino and the combined neutrino and antineutrino samples is presented in Tab. VIII relative to the MC beam prediction. The average K^+ energy and angle for the combined neutrino and antineutrino samples are reported in Tab. IX.

TABLE VIII. K^+ fit results for the rate and production relative to the MC beam prediction for the neutrino, antineutrino and combined neutrino and antineutrino samples including the final χ^2/dof obtained from the K^+ production fit for NUANCE. Errors include statistical and systematic errors. The neutrino cross-section normalizations are held at the minimized values as listed in Table VII and are relative to the NUANCE predictions.

	ν-mode	$\bar{\nu}$-mode	Combined ν+$\bar{\nu}$ mode
K^+ Prod.	0.89±0.13	0.54±0.33	0.85±0.12
K^+ Rate	0.94±0.12	0.54±0.31	0.88±0.11
χ^2/dof (Prod.)	47.8/45	18.5/27	67.3/79

TABLE IX. Measured $\frac{d^2\sigma}{dpd\Omega}$, mean energy, and mean angle (with respect to proton beam direction) for the selected K^+ in neutrino, antineutrino, and the combined neutrino and antineutrino samples using NUANCE. Errors on the mean energy and mean angle values correspond to the RMS of the relative distributions.

	E_{K^+} (GeV)	θ_{K^+}(degree)	$\frac{d^2\sigma}{dpd\Omega}$ (mb/(GeV/c × sr)
ν-mode	3.8±1.2	4.1±2.0	5.77±0.83
$\bar{\nu}$-mode	4.3±1.2	2.0±1.5	3.18±1.94
ν + $\bar{\nu}$-mode	3.9±1.0	3.7±1.6	5.34±0.76

The K^+ fit results for the production double differential cross-section in neutrino mode and antineutrino mode, though consistent, do not have to agree on the

same central value. The sample of K^+ events selected in antineutrino mode has higher energy and lower angle with respect to the ones selected in neutrino mode as shown in Tab. IV and in Tab. VI.

The values for $\frac{d^2\sigma}{dpd\Omega}$ for the neutrino, antineutrino, and combined mode results are given in Tab. IX along with the mean energy and angles for the corresponding K^+ samples. These values are obtained multiplying the measured K^+ production in Tab. VIII by the MC beam prediction in Eq. 1.

The reconstructed muon angular distribution for the SciBar 1, 2 and 3-Track Sample rescaled using the fit results are shown in Fig. 12 for neutrino mode and in Fig. 13 for antineutrino mode.

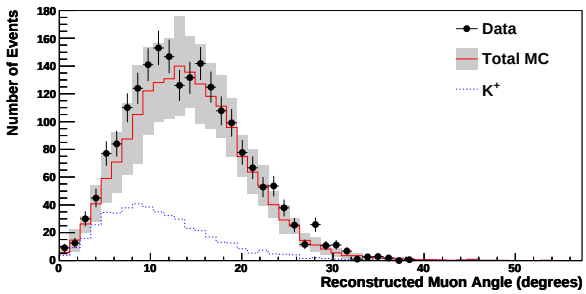

(a) 1-Track Sample

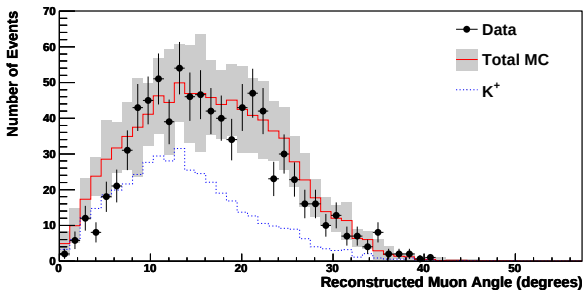

(b) 2-Track Sample

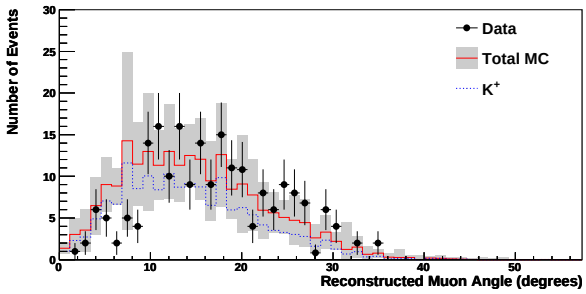

(c) 3-Track Sample

FIG. 12. Reconstructed muon angle for the SciBar 1-Track, 2-Track, and 3-Track samples after the fit in neutrino mode running for NUANCE. The K^+ production weight and the cross-section values in Table VII have been applied to the NUANCE MC predictions.

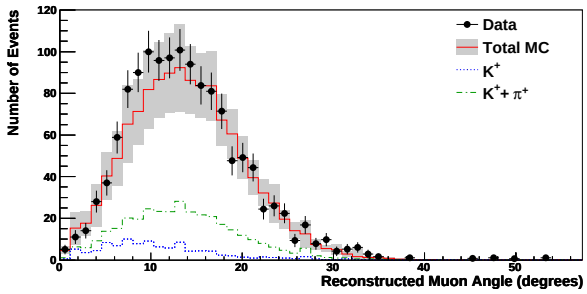

(a) 1-Track Sample

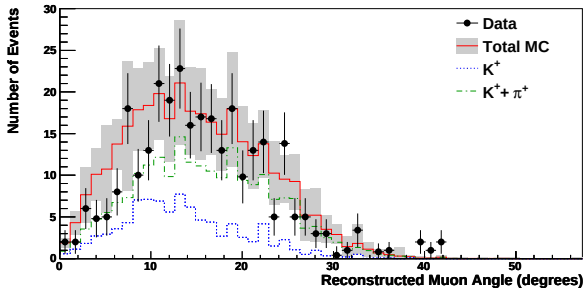

(b) 2-Track Sample

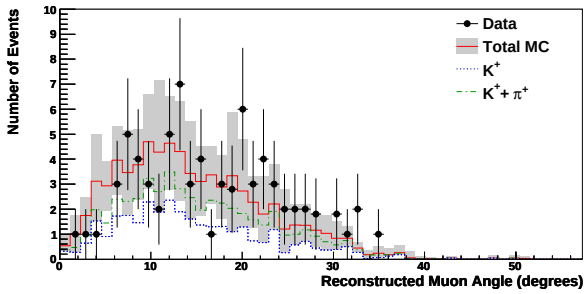

(c) 3-Track Sample

FIG. 13. Reconstructed muon angle for the SciBar 1-Track, 2-Track, and 3-Track samples after the fit in antineutrino mode running for NUANCE. The K^+ production weight and the cross-section values in Table VII have been applied to the NUANCE MC.

VII. CONCLUSION

In summary, we have made a measurement of the kaon production rate and cross section for 8 GeV protons on a Be target in the Fermilab BNB using high-energy muon neutrino events observed in the SciBooNE detector. SciBooNE's full neutrino (antineutrino) data set, corresponding to 0.99×10^{20} (1.51×10^{20}) POT, is used. The primary measurement uses the NUANCE interactions simulation and can be directly applied to the MiniBooNE oscillation analysis [20] which used that simulation. A comparison of the results obtained with the NEUT neutrino interaction simulation gives similar results (see Appendix B).

The analysis of the neutrino and antineutrino mode data are summarized in Tab. VIII. Performing the analysis on the neutrino and antineutrino mode data sets yields the following measurement for $\frac{d^2\sigma}{dpd\Omega}$ for the $p + Be \rightarrow K^+ + X$ at the mean K^+ energy of 3.9 GeV and angle 3.7 degrees:

$$\frac{d^2\sigma}{dpd\Omega} = (5.34 \pm 0.76)\ mb/(GeV/c \times sr). \quad (5)$$

The same analysis is also performed using the NEUT simulation giving the results reported in Tab. XV and the result is: $\frac{d^2\sigma}{dpd\Omega} = (5.49 \pm 0.79)\ mb/(GeV/c \times sr)$. As seen, the two simulations give very similar values (within 2.5%) and demonstrate the independency of the result with respect to the underlying neutrino cross-sections and nuclear models that are different between NUANCE and NEUT.

Applying these measurements will significantly reduce the systematic uncertainty associated with the measured ν_e background in MiniBooNE, which is a major source of uncertainty in the previously published ν_e oscillation appearance result [5] where the MiniBooNE collaboration used a conservative 40% error for the K^+ flux uncertainty. The K^+ rates (production×neutrino cross section) obtained using this analysis are:

$$K^+\ Rate = 0.85 \pm 0.11,$$

for both NUANCE and NEUT. In addition, this measurement of K^+ production in the 3.9 GeV energy region is a validation of the K^+ production predicted by the modified Feynman Scaling model [6] used in the BNB MC, which is based on K^+ production measurements at higher energies. The addition of this measurement in future fits to this model should reduce the systematic uncertainty associated with K^+ production in low energy neutrino beams.

VIII. ACKNOWLEDGMENT

We acknowledge the Physics Department at Chonnam National University, Dongshin University, and Seoul National University for the loan of parts used in SciBar and the help in the assembly of SciBar. We wish to thank the Physics Departments at the University of Rochester and Kansas State University for the loan of Hamamatsu PMTs used in the MRD. We gratefully acknowledge support from Fermilab as well as various grants, contracts and fellowships from the MEXT and JSPS (Japan), the INFN (Italy), the Ministry of Science and Innovation and CSIC (Spain), the STFC (UK), and the DOE and NSF (USA). This work was supported by MEXT and JSPS with the Grant-in-Aid for Scientific Research A 19204026, Young Scientists S 20674004, Young Scientists B 18740145, Scientific Research on Priority Areas "New Developments of Flavor Physics", and the global COE program "The Next Generation of Physics, Spun from Universality and Emergence". The project was supported by the Japan/U.S. Cooperation Program in the field of High Energy Physics and by JSPS and NSF under the Japan-U.S. Cooperative Science Program.

Appendix A: Cross-Section Fit Details

In this section we will describe the details of the cross-section fit used in the χ^2 minimization as described in Sec. VI, Eq. 4. The cross-sections described in Sec. II D have been measured in the past few years with high precision by the MiniBooNE collaboration [2, 38–40].

Eq. A1 and Eq. A2 are used to predict the number of neutrino events in bin i in case the fit is performed to measure the K^+ production or the K^+ rate. Slightly different equations, Eq. A3 and Eq. A4 are used in the antineutrino mode fit. $R^{Prod.}_{K^+}$ and $R^{Rate}_{K^+}$ are the fit parameters for the K^+ production and K^+ rate.

We use different normalization factors depending on the neutrino parent and on the interaction type. The normalization factors depend on the neutrino parent (K^+, π^+, π^-) and on the interaction types (QE, 1π, and Other). For K^+ production, the R^{QE}_ν and $R^{1\pi}_\nu$ is applied to both the K^+ and π^+ while for K^+ rate, the R^{QE}_ν and $R^{1\pi}_\nu$ is applied to only the π^+ (the neutrino cross-sections are implicit in the K^+ normalization itself). The reason we use the same normalization factors for neutrinos coming from π^+ and K^+ is because we assume no dependence in the cross-section at high energy (> 2 GeV) from the neutrino parent. We apply different normalization factors between neutrino and antineutrino mode running for neutrinos from CCQE and CC1π interaction types to correctly take into account the MiniBooNE measurement [40] on the different neutrino flux prediction in antineutrino mode running. We use R^{QE}_ν and $R^{1\pi}_\nu$ for neutrino mode running and R'^{QE}_ν and $R'^{1\pi}_\nu$ for antineutrino mode running. We do not apply any rescaling to all the other neutrino interaction types. For neutrino mode running, we do not rescale any interactions coming from antineutrinos due to the very small contamination of antineutrinos.

$$\begin{aligned} &N_i^{pred}|_{Prod.} = \\ &R^{Prod.}_{K^+} \times (R^{QE}_\nu \times N_i^{K^+_{QE}} + R^{1\pi}_\nu \times N_i^{K^+_{1\pi}} + N_i^{K^+_{Other}}) \\ &+ R^{QE}_\nu \times N_i^{\pi^+_{QE}} + R^{1\pi}_\nu \times N_i^{\pi^+_{1\pi}} + N_i^{\pi^+_{Other}} \\ &+ N_i^{\pi^-_{QE}} + N_i^{\pi^-_{1\pi}} + N_i^{\pi^-_{Other}} + N_i^{Other} \end{aligned} \quad (A1)$$

$$\begin{aligned} &N_i^{pred}|_{Rate} = R^{Rate}_{K^+} \times (N_i^{K^+_{QE}} + N_i^{K^+_{1\pi}} + N_i^{K^+_{Other}}) \\ &+ R^{QE}_\nu \times N_i^{\pi^+_{QE}} + R^{1\pi}_\nu \times N_i^{\pi^+_{1\pi}} + N_i^{\pi^+_{Other}} \\ &+ N_i^{\pi^-_{QE}} + N_i^{\pi^-_{1\pi}} + N_i^{\pi^-_{Other}} + N_i^{Other} \end{aligned} \quad (A2)$$

For antineutrino mode running, we applied additional normalization factors to take into account neutrinos produced by π^- as shown in Eq. A3 and Eq. A4.

$$
\begin{aligned}
&M_p^{pred}|_{Prod.} = \\
&R_{K^+}^{Prod.} \times (R_\nu^{'QE} \times M_p^{K^+_{QE}} + R_\nu^{'1\pi} \times M_p^{K^+_{1\pi}} + M_p^{K^+_{Other}}) \\
&+ R_\nu^{'QE} \times M_p^{\pi^+_{QE}} + R_\nu^{'1\pi} \times M_p^{\pi^+_{1\pi}} + M_p^{\pi^+_{Other}} \\
&+ R_{\bar{\nu}}^{QE} \times M_p^{\pi^-_{QE}} + R_{\bar{\nu}}^{1\pi} \times M_p^{\pi^-_{1\pi}} + M_p^{\pi^-_{Other}} \\
&+ M_p^{Other}
\end{aligned} \tag{A3}
$$

$$
\begin{aligned}
&M_p^{pred}|_{Rate} = R_{K^+}^{Rate} \times (M_p^{K^+_{QE}} + M_p^{K^+_{1\pi}} + M_p^{K^+_{Other}}) \\
&+ R_\nu^{'QE} \times M_p^{\pi^+_{QE}} + R_\nu^{'1\pi} \times M_p^{\pi^+_{1\pi}} + M_p^{\pi^+_{Other}} \\
&+ R_{\bar{\nu}}^{QE} \times M_p^{\pi^-_{QE}} + R_{\bar{\nu}}^{1\pi} \times M_p^{\pi^-_{1\pi}} + M_p^{\pi^-_{Other}} \\
&+ M_p^{Other}
\end{aligned} \tag{A4}
$$

Additional pull terms are added to the fit when we fit the K^+ normalization factors and the neutrino cross-sections. We add a pull term for each cross-section weight (6 terms total). These pull terms are then removed when performing the final χ^2 minimization, and the cross section values are fixed at their best fit values. Each of the pull terms is of the form $\frac{(R_{CS}-\mu)^2}{\sigma^2}$, where R_{CS} is the cross-section best fit value, μ is the cross-section initial value, and σ is the cross-section uncertainty.

In the case of the antineutrino mode fit for the NUANCE MC we use a larger $R_{\bar{\nu}}^{CCQE}$ and $R_{\bar{\nu}}^{1\pi}$ with respect to the central fit values to get a better agreement between data and MC for the SciBar 1-Track sample as shown in Fig. 9. For all other pull terms, μ is set at 1.0 with a 30% uncertainty. A summary of the cross-section best fit values is in Tab. VII for NUANCE MC and in Tab. XII for NEUT MC. The variations in these normalization factors for the neutrino and antineutrino cross-sections are well within the cross-section systematic uncertainties and the cross-section best fit values agree well with the cross-section measurements performed by the MiniBooNE collaboration [38–40, 40].

Appendix B: K^+ Measurements using NEUT

In the SciBooNE experiment, neutrino interactions with carbon and hydrogen in the SciBar detector are also simulated by the NEUT [17, 18] program library.

The measurements presented in Sec. III and Sec. IV are computed with assumptions on the underlying neutrino cross sections and nuclear models. Due to that, we have repeated our analysis using NEUT [17, 18] as neutrino interactions Monte Carlo. The analysis is performed in the same way as for the NUANCE MC. The reconstructed muon angle distributions for the SciBar 1, 2 and 3-Track samples are shown in Fig. 14 for the neutrino mode analysis and in Fig. 15 for the antineutrino mode analysis.

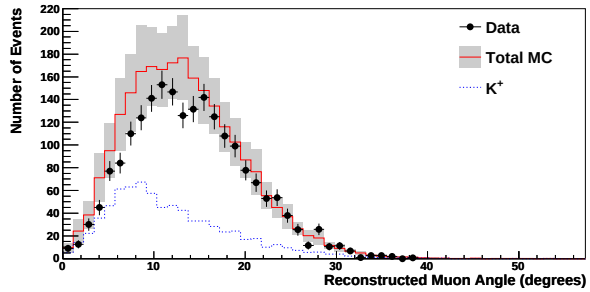

(a) 1-Track Sample

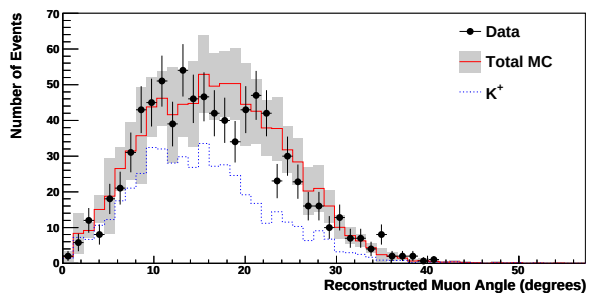

(b) 2-Track Sample

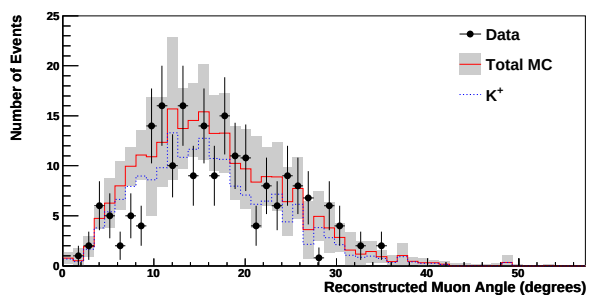

(c) 3-Track Sample

FIG. 14. Reconstructed muon angle for the SciBar 1-Track, 2-Track, and 3-Track samples in neutrino mode running for data and NEUT MC. The background contributions from K^- and K_L^0 are very small but included in the MC histogram.

NEUT and NUANCE parameters are summarized in Tab. X. The different parameter values result in different neutrino cross section predictions between the two and the differences are more in how the two Monte Carlos implement nuclear and cross section models. The total interaction numbers predicted by NEUT are summarized in Tab. XI.

The difference in the parameter choices (Tab. X), leads to NEUT predicting a larger QE and single pion rate than NUANCE. This difference in QE rate comes largely from the choice of κ values, and the difference in single pion rate can be largely accounted for by the difference in

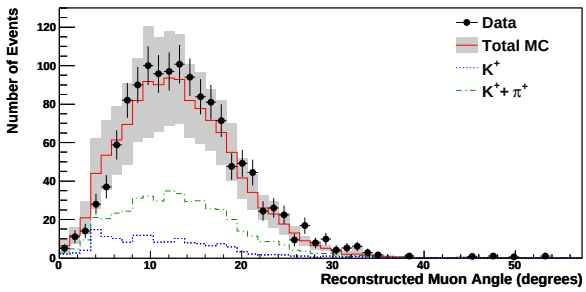

(a) 1-Track Sample

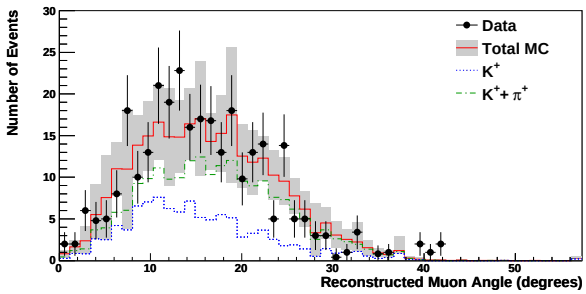

(b) 2-Track Sample

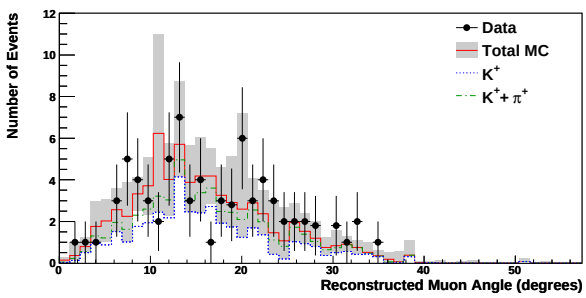

(c) 3-Track Sample

FIG. 15. Reconstructed muon angle for the SciBar 1-Track, 2-Track, and 3-Track samples in antineutrino mode running for data and NEUT MC. The background contributions from K^- and K^0_L are small but included in the MC histogram.

TABLE X. Parameter used for Neutrino interaction simulation.

Parameter	NEUT	NUANCE
p_F	217 MeV	220 MeV
E_B	25 MeV	34 MeV
M_A^{QE}-C	1.21 GeV	1.234 GeV
M_A^{QE}-H	1.0 GeV	1.0 GeV
κ	1.00	1.022
$M_A^{1\pi}$	1.21 GeV	1.10 GeV
$M_A^{coherent}$	1.03 GeV	1.03 GeV
$M_A^{N\pi}$	(DIS)	1.3 GeV

$M_A^{1\pi}$ assumptions. CC-QE interactions, which are implemented using the Smith and Moniz model [21], are the dominant interaction in the SciBooNE neutrino energy range. The nucleons are treated as quasi-free particles and the Fermi motion of nucleons along with the Pauli exclusion principle is taken into account. The Fermi surface momentum (p_F) for carbon is set to 217(220) MeV/c and the nuclear potential (E_B) is set to 25(34) MeV/c for NEUT(NUANCE), as extracted from electron scattering data [22]. The default binding energy in NUANCE is somewhat higher than in NEUT because it additionally accounts for neutrino vs. electron scattering differences [23]. With regards to the vector form factor, NEUT uses a dipole form with a vector mass of 0.84 GeV/c^2, while NUANCE uses the BBA-2003 form factor [24]. A dipole form is used for the axial form factor with an adjustable axial mass, M_A^{QE}, for both NEUT and NUANCE. The values of $M_A^{QE} = 1.21$ GeV/c^2 and $\kappa = 1.000$ (i.e. no additional Pauli blocking adjustment) are used in NEUT, and $M_A^{QE} = 1.234$ GeV/c^2 and $\kappa = 1.022$ are used in NUANCE [23]. The same Fermi momentum distribution and nuclear potential are used in all other neutrino-nucleus interactions except for resonant π production.

TABLE XI. The expected number of events in each neutrino interaction estimated by NEUT at the SciBooNE detector location with the neutrino beam exposure of 0.99×10^{20} protons on target for neutrino mode and of 1.51×10^{20} for antineutrino mode. The 9.8 ton fiducial volume of the SciBar detector is assumed. CC and NC interactions are abbreviated as CC and NC, respectively.

	NEUT	
Interaction	# Events neutrino mode	# Events antineutrino mode
CC QE	50,330	18,804
CC single-π	27,836	7,350
CC coh. π	1,692	1,308
CC DIS+Other	6,445	1,760
NC	35,153	13,194

The resonant production of single pion, kaon, and eta mesons, as described by the model of Rein and Sehgal (RS) [26], is implemented with axial-vector form factors formalized to be dipole with $M_A^{1\pi} = 1.21$ GeV/c^2 for NEUT and $M_A^{1\pi} = 1.10$ GeV/c^2 for NUANCE. Resonance decays leading to multi-pion final states are also included in the NUANCE model as described in Sec. II D. In NEUT, multi-pion production is simulated as deep inelastic scattering (DIS) and the RS model is not used. Multi-hadron final states are simulated by two models: a custom-made program [41] for events with W between 1.3 and 2.0 GeV/c^2 and PYTHIA/JETSET [42] for events with W larger than 2 GeV/c^2. The pion multiplicity is additionally restricted to be greater than one for $1.3 < W < 2$ GeV/c^2 to avoid double-counting sources of single pion production. In NUANCE, the DIS contribu-

tion slowly increases for W values starting at 1.7 GeV and becomes the only source of neutrino interactions above $W > 2$ GeV.

The total and inelastic pion-nucleon cross sections are treated differently in NEUT and NUANCE. In NEUT they are from the original Rein and Sehgal publication [28, 29] while in NUANCE, they are obtained from fits to PDG data [43] and implemented as a function of pion energy with an additional rescale of the NC and CC coherent pion production cross section.

Intra nuclear interactions are simulated differently as well: more details can be found for both NEUT and NUANCE in [16, 19].

The results obtained for the cross-section best fit values using NEUT in the neutrino and antineutrino mode are summarized in Tab. XII.

TABLE XII. Summary of the fit results for the cross-section normalization factors as described in Appendix A with respect to NEUT predictions. The top four values are cross section normalization values for ν_μ and $\bar{\nu}_\mu$ coming from π^+ and K^+ while the last two are normalization factors for $\bar{\nu}_\mu$ coming from π^-.

π^+/K^+		Fit Value
	CCQE in ν mode	0.92±0.13
	CCQE in $\bar{\nu}$ mode	1.05±0.25
	CC1π in ν mode	1.12±0.25
	CC1π in $\bar{\nu}$ mode	0.94±0.27
π^-		
	CCQE in $\bar{\nu}$ mode	1.01±0.30
	CC1π in $\bar{\nu}$ mode	1.01±0.30

The mean energy and mean angle (with respect to proton beam direction) for the selected K^+ and the mean energy for ν_μ from the selected K^+ in each of the three samples, for both neutrino mode running and antineutrino mode running, are summarized in Tab. XIII and Tab. XIV. A summary of the fit results obtained for the K^+ production and rate separately for neutrino, antineutrino and the combined neutrino and antineutrino samples is presented in Tab. XV relative to the MC beam prediction.

TABLE XIII. Neut MC predicted mean energy and mean angle (with respect to the proton beam direction) for the selected K^+ samples and predicted MC energy for the selected ν_μ from K^+ in the three SciBar samples in neutrino mode running. Errors correspond to the RMS of the relative distributions.

	E_{K^+} (GeV)	θ_{K^+}(degree)	E_{ν_μ} (GeV)
1-Track	3.6±1.2	4.2±2.0	3.1±1.0
2-Track	3.9±1.2	4.0±2.0	3.3±1.0
3-Track	4.2±1.1	3.6±1.9	3.6±0.9

TABLE XIV. Neut MC predicted mean energy and mean angle (with respect to the proton beam direction) for the selected K^+ samples and predicted MC energy for the selected ν_μ from K^+ for the three SciBar samples in antineutrino mode running. Errors correspond to the RMS of the relative distributions.

	E_{K^+} (GeV)	θ_{K^+}(degree)	E_{ν_μ} (GeV)
1-Track	4.1±1.3	2.2±1.6	3.1±1.1
2-Track	4.3±1.2	1.7±1.2	3.4±1.0
3-Track	4.7±1.1	1.6±1.0	3.8±1.0

The average K^+ energy and angle for the combined neutrino and antineutrino samples are reported in Tab. XVI.

TABLE XV. K^+ fit results for the rate and production relative to the MC beam prediction for the neutrino, antineutrino and combined neutrino and antineutrino samples including the final χ^2/dof obtained from the K^+ production fit for NEUT. Errors include statistical and systematic errors. The neutrino cross-section normalizations are held at the minimized values as listed in Table XII and are relative to the NEUT predictions.

	ν-mode	$\bar{\nu}$-mode	Combined ν+$\bar{\nu}$ mode
K^+ Prod.	0.90±0.14	0.77±0.33	0.87±0.12
K^+ Rate	0.92±0.12	0.76±0.30	0.88±0.11
χ^2/dof (K^+ Prod.)	40.6/45	17.7/26	58.9/77

TABLE XVI. Measured $\frac{d^2\sigma}{dpd\Omega}$, mean energy, and mean angle (with respect to proton beam direction) for the selected K^+ in neutrino, antineutrino, and the combined neutrino and antineutrino samples using NEUT. Errors on the mean energy and mean angle values correspond to the RMS of the relative distributions.

	E_{K^+} (GeV)	θ_{K^+}(degree)	$\frac{d^2\sigma}{dpd\Omega}$ (mb/(GeV/c × sr)
ν-mode	3.8±1.2	4.0±2.0	5.85±0.90
$\bar{\nu}$-mode	4.3±1.3	1.9±1.4	4.59±1.97
ν + $\bar{\nu}$-mode	3.9±1.0	3.7±1.6	5.49±0.79

The values for $\frac{d^2\sigma}{dpd\Omega}$ for the neutrino, antineutrino, and combined mode results are given in Tab. XVI along with the mean energy and angles for the corresponding K^+ samples. These values are obtained multiplying the measured K^+ production in Tab. XV by the MC beam prediction in Eq. 1.

The reconstructed muon angle distributions for the SciBar 1, 2 and 3-Track samples rescaled using the fit results are shown in Fig. 16 for the neutrino mode analysis and in Fig. 17 for the antineutrino mode analysis.

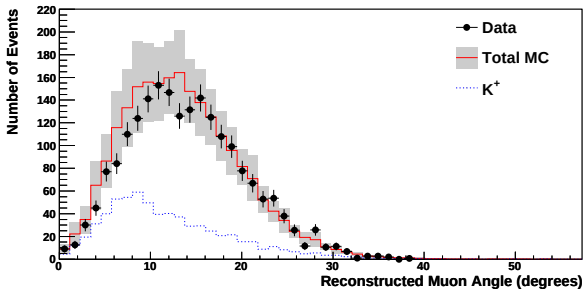

(a) 1-Track Sample

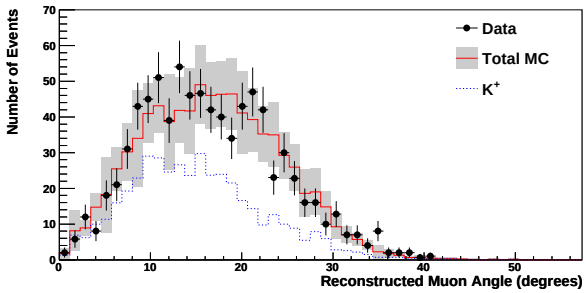

(b) 2-Track Sample

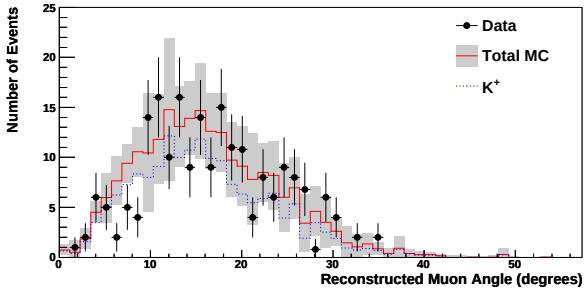

(c) 3-Track Sample

FIG. 16. Reconstructed muon angle for the SciBar 1-Track, 2-Track, and 3-Track samples in neutrino mode running for data and the NEUT MC. The K^+ production weight and the cross-section central values in Table XII have been applied to the NEUT predictions.

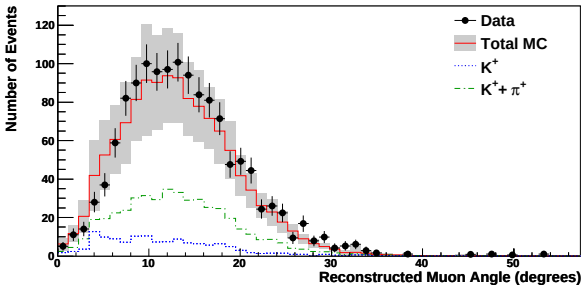

(a) 1-Track Sample

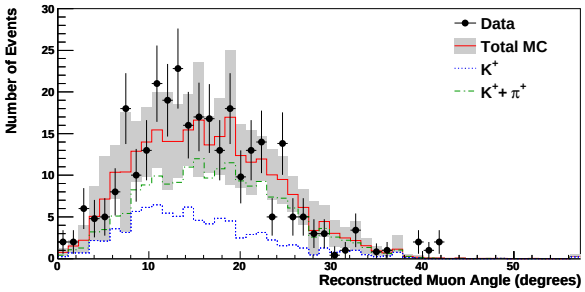

(b) 2-Track Sample

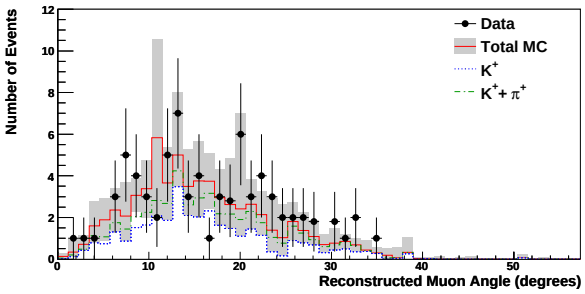

(c) 3-Track Sample

FIG. 17. Reconstructed muon angle for the SciBar 1-Track, 2-Track, and 3-Track samples in antineutrino mode running for data and NEUT MC. The K^+ production weight and the cross-section central values in Table XII have been applied to the NEUT predictions.

[1] R. P. Feynman. Very high-energy collisions of hadrons. *Phys. Rev. Lett.*, 23(24):1415–1417, Dec 1969.

[2] A. A. Aguilar-Arevalo et al. The Neutrino Flux prediction at MiniBooNE. *Phys. Rev.*, D79:072002, 2009.

[3] K. Hiraide. The SciBar detector at FNAL booster neutrino experiment. *Nucl. Phys. Proc. Suppl.*, 159:85–90, 2006.

[4] Mitchell Soderberg. MicroBooNE: A New Liquid Argon Time Projection Chamber Experiment. *AIP Conf. Proc.*, 1189:83–87, 2009.

[5] A. A. Aguilar-Arevalo et al. A Search for Electron Antineutrino Appearance at the $\Delta m^2 \sim 1$ eV^2 Scale. *Phys. Rev. Lett.*, 103:111801, 2009.

[6] M. Shaevitz, C. Mariani, et al. Parameterizing the p-be k$^+$ production cross section using a feynman scaling function, 2010. PRD in preparation.

[7] J. R. Sanford and C. L. Wang. BNL Internal Report number BNL 11479.

[8] J.R. Sanford and C.L. Wang, 1967. BNL Note No. 11299.

[9] M. G. Catanesi et al. Measurement of the production cross-section of positive pions in the collision of 8.9 GeV/c protons on beryllium. *Eur. Phys. J.*, C52:29–53, 2007.

[10] N. V. Mokhov et al. MARS Code Developments. *arXiv:nucl-th/9812038*, 1998.

[11] Y. Nakajima et al. Measurement of inclusive charged current interactions on carbon in a few-GeV neutrino beam. *Phys. Rev.*, D83:012005, 2011.

[12] K. Nitta et al. The K2K SciBar detector. *Nucl. Instrum. Meth.*, A535:147–151, 2004.

[13] M. Yoshida et al. Development of the readout system for the K2K SciBar detector. *IEEE Trans. Nucl. Sci.*, 51:3043–3046, 2004.

[14] C. Mariani. EC detector at SciBooNE. *J. Phys. Conf. Ser.*, 160:012035, 2009.

[15] A. Heikkinen, N. Stepanov, and J. P. Wellisch. Bertini intra-nuclear cascade implementation in Geant4. *arXiv:nucl-th/0306008*, 2003.

[16] K. Hiraide et al. Search for Charged Current Coherent Pion Production on Carbon in a Few-GeV Neutrino Beam. *Phys. Rev.*, D78:112004, 2008.

[17] Y. Hayato. NEUT. *Nucl. Phys. Proc. Suppl.*, 112:171–176, 2002.

[18] G. Mitsuka. NEUT. *AIP Conf. Proc.*, 981:262–264, 2008.

[19] D. Casper. The nuance neutrino physics simulation, and the future. *Nucl. Phys. Proc. Suppl.*, 112:161–170, 2002.

[20] A. A. Aguilar-Arevalo et al. A Search for electron neutrino appearance at the $\Delta m^2 \sim 1$eV^2 scale. *Phys. Rev. Lett.*, 98:231801, 2007.

[21] R.A. Smith and E.J. Moniz. Neutrino reactions on nuclear targets. *Nuclear Physics B*, 43:605 – 622, 1972.

[22] E. J. Moniz et al. Nuclear fermi momenta from quasielastic electron scattering. *Phys. Rev. Lett.*, 26:445–448, 1971.

[23] A. A. Aguilar-Arevalo et al. Measurement of muon neutrino quasi-elastic scattering on carbon. *Phys. Rev. Lett.*, 100:032301, 2008.

[24] H. S. Budd, A. Bodek, and J. Arrington. Modeling quasi-elastic form factors for electron and neutrino scattering. *hep-ex/0308005*, 2003.

[25] A. A. Aguilar-Arevalo et al. First Measurement of the Muon Neutrino Charged Current Quasielastic Double Differential Cross Section. *Phys. Rev.*, D81:092005, 2010.

[26] D. Rein and L. M. Sehgal. Neutrino Excitation of Baryon Resonances and Single Pion Production. *Ann. Phys.*, 133:79, 1981.

[27] D. Rein. Angular Distribution in neutrino induced single pion production processes. *Z. Phys.*, C35:43–64, 1987.

[28] D. Rein and L. M. Sehgal. Coherent π^0 Production in Neutrino Reactions. *Nucl. Phys.*, B223:29, 1983.

[29] D. Rein and L. M. Sehgal. PCAC and the Deficit of Forward Muons in π^+ Production by Neutrinos. *Phys. Lett.*, B657:207–209, 2007.

[30] M. Gluck, E. Reya, and A. Vogt. Dynamical parton distributions revisited. *Eur. Phys. J.*, C5:461–470, 1998.

[31] A. Bodek and U. K. Yang. Modeling neutrino and electron scattering cross sections in the few GeV region with effective LO PDFs. *hep-ex/0308007*, 2003.

[32] A. Glazov, I. Kisel, E. Konotopskaya, and G. Ososkov. Filtering tracks in discrete detectors using a cellular automaton. *Nucl. Instrum. Meth.*, A329:262–268, 1993.

[33] K. Hiraide. *A Study of Charged Current Single Charged Pion Productions on Carbon in a Few-GeV Neutrino Beam*. PhD thesis, Kyoto University, 2009. FERMILAB-THESIS-2009-02.

[34] A. Bodek, S. Avvakumov, R. Bradford, and Howard Scott Budd. Extraction of the Axial Nucleon Form Factor from Neutrino Experiments on Deuterium. *J. Phys. Conf. Ser.*, 110:082004, 2008.

[35] A. Rodriguez et al. Measurement of single charged pion production in the charged-current interactions of neutrinos in a 1.3 GeV wide band beam. *Phys. Rev.*, D78:032003, 2008.

[36] T. Kitagaki et al. Charged current exclusive pion production in neutrino deuterium interactions. *Phys. Rev.*, D34:2554–2565, 1986.

[37] D. Day et al. Study of neutrino d charged current two pion production in the threshold region. *Phys. Rev.*, D28:2714–2720, 1983.

[38] A. A. Aguilar-Arevalo et al. Measurement of muon neutrino quasi-elastic scattering on carbon. *Phys. Rev. Lett.*, 100:032301, 2008.

[39] A. A. Aguilar-Arevalo et al. Measurement of Neutrino-Induced Charged-Current Charged Pion Production Cross Sections on Mineral Oil at $E_\nu \sim 1$ GeV. *Phys. Rev.*, D83:052007, 2011.

[40] A. A. Aguilar-Arevalo et al. Measurement of the neutrino component of an anti-neutrino beam observed by a non-magnetized detector. *arXiv:1102.1964*, 2011.

[41] M. Nakahata et al. Atmospheric Neutrino Background and Pion Nuclear Effect for Kamioka Nucleuon Decay Experiment. *J. Phys. Soc. Jap.*, 55:3786, 1986.

[42] T. Sjostrand. High-energy physics event generation with PYTHIA 5.7 and JETSET 7.4. *Comput. Phys. Commun.*, 82:74–90, 1994.

[43] K. Nakamura and Particle Data Group. Review of particle physics. *Journal of Physics G: Nuclear and Particle Physics*, 37(7A):075021, 2010.